LETTER

https://doi.org/10.1038/s41586-019-1018-5

Small-molecule ion channels increase host defences in cystic fibrosis airway epithelia

Katrina A. Muraglia[1], Rajeev S. Chorghade[2], Bo Ram Kim[3], Xiao Xiao Tang[3], Viral S. Shah[3], Anthony S. Grillo[2], Page N. Daniels[1], Alexander G. Cioffi[1], Philip H. Karp[3], Lingyang Zhu[2], Michael J. Welsh[3,4] & Martin D. Burke[1,2,5,6,7]*

Loss-of-function mutations in the cystic fibrosis transmembrane conductance regulator (CFTR) compromise epithelial HCO_3^- and Cl^- secretion, reduce airway surface liquid pH, and impair respiratory host defences in people with cystic fibrosis[1–3]. Here we report that apical addition of amphotericin B, a small molecule that forms unselective ion channels, restored HCO_3^- secretion and increased airway surface liquid pH in cultured airway epithelia from people with cystic fibrosis. These effects required the basolateral Na^+, K^+-ATPase, indicating that apical amphotericin B channels functionally interfaced with this driver of anion secretion. Amphotericin B also restored airway surface liquid pH, viscosity, and antibacterial activity in primary cultures of airway epithelia from people with cystic fibrosis caused by different mutations, including ones that do not yield CFTR, and increased airway surface liquid pH in *CFTR*-null pigs in vivo. Thus, unselective small-molecule ion channels can restore host defences in cystic fibrosis airway epithelia via a mechanism that is independent of CFTR and is therefore independent of genotype.

Increasing anion secretion through CFTR channels that bear specific mutations improves airway host defences and lung function in people with cystic fibrosis (CF)[1,4,5]. However, not all CFTR mutations are amenable to this approach[6]. Small-molecule ion channels that operate independently of CFTR to promote anion secretion might circumvent these limitations. Multiple studies have demonstrated that peptide or small-molecule ion channels, transporters and carriers can promote Cl^- transport in CFTR-deficient cells and/or changes in short-circuit current or potential in CFTR-deficient epithelia[7–10]. However, it has remained unclear whether this approach can improve airway host defences.

Recent studies have demonstrated that HCO_3^- secretion may enhance airway host defences[2,3,11] by increasing airway surface liquid (ASL) pH[3], decreasing ASL viscosity[3,12], increasing activity of antimicrobial factors[3], maintaining ASL volume homoeostasis[13], counteracting local environment acidification by *Pseudomonas aeruginosa*[14] and dissipating proton-motive forces in bacteria[15]. The electrochemical gradient across the apical membrane favours HCO_3^- secretion; HCO_3^- is accumulated intracellularly through the integrated activity of Na^+, K^+-ATPase, H^+, K^+-ATPase and K^+ channels, Na^+, HCO_3^- transporters, and Na^+/H^+ antiporters, as well as carbonic anhydrase[3,16]. Thus, when CFTR opens, HCO_3^- flows into the ASL, increasing ASL pH. In the absence of CFTR, intracellular HCO_3^- concentration is maintained[17], and this gradient for HCO_3^- exit persists or is likely to increase as ASL pH falls. We reasoned that the electrochemical gradient for HCO_3^- across the apical membrane of CF epithelia at steady state may permit even an unselective small-molecule HCO_3^- transporter to increase basolateral-to-apical HCO_3^- flux and thus airway host defences. An unselective small-molecule iron transporter was sufficient to restore haemoglobinization in cells and animals that are deficient in iron-transport proteins, and this tolerance for lack of selectivity was linked to iron gradients across membranes that normally host the missing proteins[18].

Amphotericin B (AmB) is a small-molecule natural product that forms monovalent ion channels that are unselective for anions versus cations. It is prescribed as an antifungal, but is markedly toxic to humans[19]. We recently found that its cytotoxicity is primarily owing to sterol extraction from membranes, and not a result of channel formation[20,21]. In the presence of lipid bilayers, AmB is likely to exist in at least two states that are in dynamic equilibrium[20,21]. The primary state is a toxic extramembranous sterol sponge, but it also exists as a membrane-embedded ion channel. Toxicity from the AmB sterol sponge only occurs when the molar ratio of AmB:sterol is greater than one[20,21]. These insights allowed the channel activity of AmB to be rationally separated from its cytotoxicity using either low concentrations of AmB that form ion channels but do not extract substantial amounts of membrane sterol (generally less than 0.5 μM in ergosterol-containing yeast, predicted to be generally less than 5 μM in cholesterol-containing mammalian cells), or by pre-complexing AmB to excess sterols[20–22]. Although AmB forms ion channels that are permeable to both cations and anions, it restored K^+ transport and growth in yeast missing the K^+-selective Trk transporters[22]. By contrast, a synthetic single-atom-deficient derivative that lacks ion-channel activity (C35deOAmB) did not restore K^+ transport and growth[20,22]. We hypothesized that, in the context of a favourable electrochemical gradient for HCO_3^- secretion, apical AmB channels would increase HCO_3^- secretion and thus ASL host defences in CF epithelium.

AmB transports monovalent anions and cations (Extended Data Fig. 1f–h, j), but it is not known whether it transports HCO_3^- specifically. We found that AmB, but not C35deOAmB, caused $H^{13}CO_3^-$ efflux in cholesterol-containing palmitoyl oleoyl phosphatidylcholine (POPC) liposomes (Extended Data Fig. 1a–e, i).

A low concentration of AmB increased ASL pH and $H^{14}CO_3^-$ secretion in CuFi-4 cultured airway epithelia, which are heterozygous for the CFTR mutations (G551D/ΔF508) (Fig. 1a, b). pH-stat experiments indicated that HCO_3^- secretion, rather than proton absorption, primarily underlies the AmB-mediated increase in ASL pH (Extended Data Fig. 2a). For comparison, we tested ivacaftor, which increases the open-state probability of CFTR[23] and improves forced expiratory volume in 1 s in people with CF carrying a G551D or other residual-function mutation in CFTR[4]. The quantitative effects of AmB on ASL pH and $H^{14}CO_3^-$ secretion were similar to those of ivacaftor (Fig. 1a, b). AmB transports both anions and cations (Extended Data Fig. 1f–j), but ASL concentrations of Na^+ and K^+ were unchanged with AmB treatment relative to vehicle-treated controls (Extended Data Fig. 2b, c). Whereas AmB is likely to mobilize ions other than HCO_3^-, we speculate that compensatory actions of other pumps, channels, carriers and the paracellular pathway may help to determine ASL ion concentrations at steady state.

[1]Department of Biochemistry, University of Illinois at Urbana-Champaign, Urbana, IL, USA. [2]Department of Chemistry, University of Illinois at Urbana-Champaign, Urbana, IL, USA. [3]Department of Internal Medicine and HHMI, Pappajohn Biomedical Institute, Roy J. and Lucille A. Carver College of Medicine, University of Iowa, Iowa City, IA, USA. [4]Department of Molecular Physiology and Biophysics, Roy J. and Lucille A. Carver College of Medicine, University of Iowa, Iowa City, IA, USA. [5]Carle Illinois College of Medicine, University of Illinois at Urbana-Champaign, Champaign, IL, USA. [6]Carl R. Woese Institute for Genomic Biology, University of Illinois at Urbana-Champaign, Champaign, IL, USA. [7]Beckman Institute for Advanced Science and Technology, University of Illinois at Urbana-Champaign, Champaign, IL, USA. *e-mail: mdburke@illinois.edu

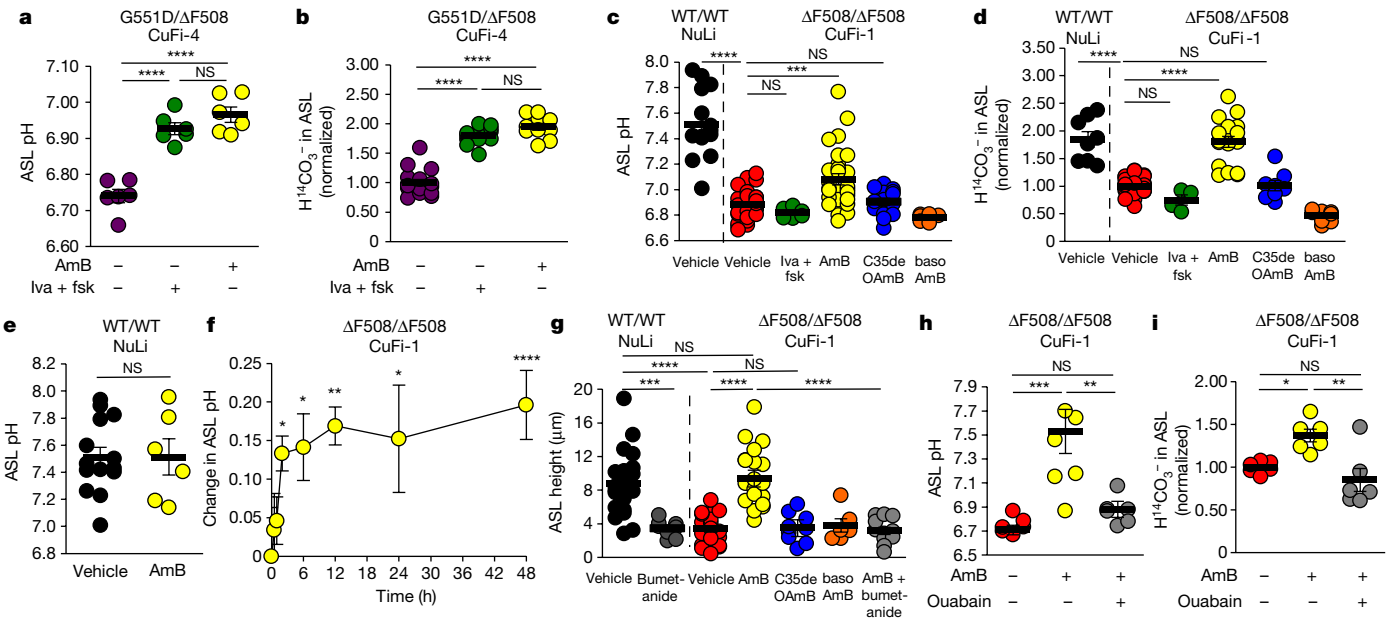

Fig. 1 | AmB increased $H^{14}CO_3^-$ secretion and ASL pH in cultured CF airway epithelia. a, Effect of ivacaftor and forskolin (Iva + fsk) or AmB on ASL pH in CuFi-4 (G551D/ΔF508) epithelia ($n = 6$). **b**, Effect of ivacaftor and forskolin ($n = 12$) or AmB ($n = 10$) on basolateral-to-apical $H^{14}CO_3^-$ secretion in CuFi-4 epithelia ($n = 16$). **c**, Effect of vehicle (perfluorocarbon-72 (FC-72)), ivacaftor and forskolin ($n = 6$), AmB ($n = 28$), C35deOAmB ($n = 14$) or basolateral AmB ($n = 6$) on ASL pH in NuLi (*CFTR*$^{+/+}$) ($n = 14$) or CuFi-1 (ΔF508/ΔF508) epithelia ($n = 37$). **d**, Effect of vehicle ($n = 37$), ivacaftor and forskolin ($n = 4$), AmB ($n = 18$), C35deOAmB ($n = 8$) or basolateral AmB ($n = 8$) on $H^{14}CO_3^-$ secretion in NuLi ($n = 8$) or CuFi-1 epithelia ($n = 37$). **e**, Effect of AmB ($n = 6$) on ASL pH in NuLi epithelia ($n = 16$). **f**, Average difference in ASL pH after AmB treatment compared to vehicle in CuFi-1 epithelia as a function of time (0, 0.5, 1, 2 and 12 h, $n = 6$; 6 h, $n = 9$; 24 h, $n = 12$; 48 h, $n = 28$). **g**, ASL height in NuLi ($n = 21$) or CuFi-1 epithelia ($n = 21$) after treatment with apical AmB ($n = 21$), C35deOAmB ($n = 9$), basolateral (baso) AmB ($n = 6$) or AmB with bumetanide ($n = 12$). **h**, **i**, ASL pH (**h**) and $H^{14}CO_3^-$ secretion (**i**) in CuFi-1 epithelia ($n = 6$) after addition of vehicle, apical AmB or AmB with ouabain. *n* is the number of biologically independent samples from at least two independent experiments with similar results. Data are mean ± s.e.m. **a**–**d**, **g**–**i**, One-way ANOVA with Tukey test for multiple comparisons. **e**, **f**, Two-sided unpaired Student's *t*-test. NS, not significant; $^*P \leq 0.05$; $^{**}P \leq 0.01$; $^{***}P \leq 0.001$; $^{****}P \leq 0.0001$. *P* are shown in the Source Data.

Ivacaftor does not correct the non-membrane-localized ΔF508 CFTR defect[23], and as expected, it failed to increase ASL pH or $H^{14}CO_3^-$ secretion in CuFi-1 (ΔF508/ΔF508) epithelia (Fig. 1c, d). By contrast, AmB, which operates independently of the CFTR protein, increased both ASL pH and $H^{14}CO_3^-$ secretion (Fig. 1c, d). No increase in ASL pH was observed with apical addition of AmB to non-CF (NuLi) epithelia (Fig. 1e). AmB was left on the epithelia throughout all the experiments described in this paper. AmB progressively increased ASL pH over 2 h, and sustained this effect for at least 48 h in these in vitro experiments (Fig. 1f). The AmB-mediated increase in $H^{14}CO_3^-$ secretion in CuFi-1 epithelia is sustained for at least seven days (Extended Data Fig. 3a–c). These results contrast with the transient increase in pH (lasting approximately 15 min)[24] produced by aerosolized $NaHCO_3$. C35deOAmB and basolateral addition of AmB did not increase ASL pH or $H^{14}CO_3^-$ secretion, suggesting that these effects are specific to apically localized AmB channels (Fig. 1c, d).

AmB-treated CuFi-1 epithelia did not respond to chemical activation of CFTR, suggesting that AmB did not promote trafficking of ΔF508 CFTR to the apical membrane (Extended Data Fig. 3d–i). Addition of AmB did not disrupt membrane integrity, as there was no difference in transepithelial electrical resistance (R_t) between CuFi-1 epithelia treated with either vehicle, low (2 μM) or high (50 μM) doses of AmB over extended timeframes (Extended Data Fig. 3j). No toxicity was observed in CuFi-1 epithelia with the same AmB doses (Extended Data Fig. 3k).

Another model of CF links ASL height to pathology[13]. At baseline, CuFi-1 epithelia had decreased ASL height compared with NuLi epithelia (Fig. 1g, Extended Data Fig. 4a, b). Apical addition of AmB increased ASL height to match that of NuLi epithelia (Fig. 1g, Extended Data Fig. 4c). Vehicle, C35deOAmB and basolateral AmB did not increase ASL height (Fig. 1g, Extended Data Fig. 4d, e). These results suggest that AmB-based channels restore ASL volume homoeostasis despite their lack of ion selectivity.

Secretion of ions through apical channels depends on an electrochemical gradient generated in large part by basolateral transport proteins. We showed that AmB-mediated growth rescue in Trk-deficient yeast is attenuated by chemical inhibition of H^+-ATPases that drive secondary K^+ influx[22]. Secretion of Cl^- through apical peptide channels in monolayers derived from a colonic cancer cell line was mitigated by blocking basolateral K^+ channels[25]. We predicted that inhibiting basolateral transport in CF airway epithelia would similarly prevent AmB-mediated anion secretion. Inhibiting the basolateral Na^+, K^+-ATPase with ouabain abolished the AmB-mediated increase in ASL pH and $H^{14}CO_3^-$ secretion in CuFi-1 epithelia (Fig. 1h, i). Inhibiting the basolateral $Na^+/K^+/2Cl^-$ co-transporter with bumetanide decreased ASL height in NuLi epithelia and abolished the AmB-mediated increase in ASL height in CuFi-1 epithelia (Fig. 1g, Extended Data Fig. 4f, g). Thus, apical AmB channels functionally interface with endogenous basolateral proteins that drive anion secretion.

We next tested whether AmB could restore key aspects of airway host defence in differentiated primary cultures of human airway epithelia. We studied epithelia from nine donors with CF representing different CFTR mutations, including some that yield no CFTR (Fig. 2a, Extended Data Fig. 5a). Apical AmB increased ASL pH by approximately 0.2 pH units (Fig. 2a), and this effect was sustained for at least 48 h (Fig. 2b). C35deOAmB and basolateral AmB did not increase ASL pH (Extended Data Fig. 5b).

ASL viscosity is increased and antibacterial activity is decreased in cultures of CF airway epithelia[3,26]. The ASL of non-CF airway epithelia has a viscosity 2.5 times that of saline[3]. Apical addition of AmB to genetically diverse primary cultures of CF epithelia decreased ASL viscosity (Fig. 2c, Extended Data Fig. 5d, h–j) to a degree that matched

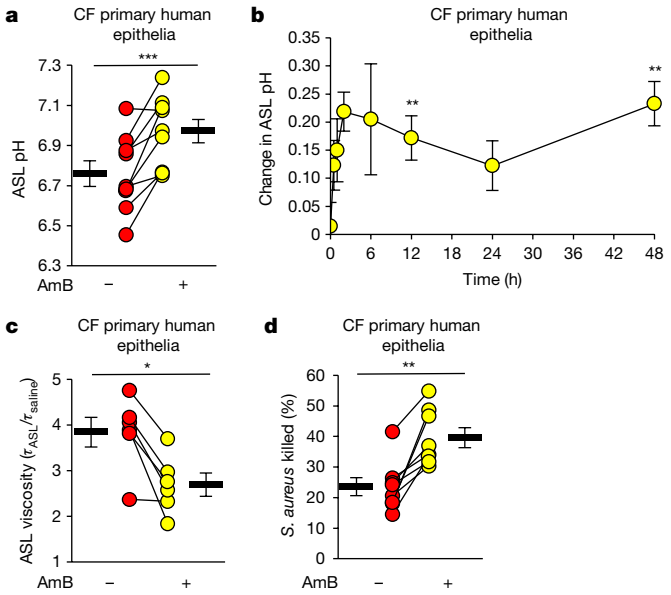

Fig. 2 | AmB improved host defences in primary cultured airway epithelia derived from genetically diverse humans with CF. a, Effect of AmB on ASL pH in primary cultured airway epithelia derived from nine humans with CF with different *CFTR* mutations ($n = 9$). **b**, Average difference in ASL pH after AmB treatment compared to vehicle treatment as a function of time (0, 0.5, 2 h, $n = 6$; 6, 12, 24 h, $n = 3$; 1, 48 h, $n = 9$). **c**, **d**, Effect of apical AmB treatment on ASL viscosity (τ_{ASL}/τ_{saline}) (**c**; $n = 6$) and ASL antibacterial activity (**d**; $n = 8$) in primary CF epithelia. Data are mean ± s.e.m. In **a**, **b**, **d**, each data point represents an average of 1–3 epithelia samples from each human donor. In **a**, **c**, **d**, n is the number of biologically independent samples from at least three independent experiments with similar results. In **b**, the same samples for each donor were measured repeatedly over time; data are from at least three independent experiments with similar results. All panels, two-sided unpaired Student's t-test. $^*P \leq 0.05$; $^{**}P \leq 0.01$; $^{***}P \leq 0.001$. P values are shown in the Source Data.

ivacaftor in primary G551D CFTR sinonasal epithelia[12]. Antimicrobial activity of ASL is reduced by about 50% in CF[3]. AmB addition nearly doubled ASL bacterial killing in CF epithelia (Fig. 2d, Extended Data Fig. 5e, f), whereas C35deOAmB had no effect (Extended Data Fig. 5f). AmB alone does not have antibacterial activity against *Staphylococcus aureus* (Extended Data Fig. 5g).

In CuFi-1 epithelia ASL pH increased and then fell with increasing concentrations of AmB (Fig. 3a). On the basis of our previous findings in yeast cells[20–22], we hypothesized that preforming a AmB–cholesterol complex would mitigate potential sterol-binding-mediated effects that could contribute to reduced efficacy at higher concentrations of AmB. We found that a preformed AmB–cholesterol (1:5) complex increased ASL pH up to the maximum concentration of AmB tested (100 μM) (Fig. 3a).

AmBisome is a liposomal formulation, approved by the US Food and Drug Administration, that contains AmB and cholesterol in a 1:2.5 ratio[27]. AmBisome caused $H^{13}CO_3^-$ efflux in liposomes (Extended Data Fig. 6a), increased ASL pH and $H^{14}CO_3^-$ secretion in CuFi-1 epithelia measured 2 h and 48 h after addition (Fig. 3b, c, Extended Data Fig. 6b, c), and increased ASL pH over a large range of AmBisome concentrations, 6–2,450 μg ml^{-1}, equivalent to 0.25–100 μM AmB (Extended Data Fig. 6c).

To assess whether AmBisome can restore ASL pH in vivo, we used a porcine model of CF[24]. The ASL pH of *CFTR*$^{-/-}$ pigs does not increase without intervention with aerosolized HCO_3^- or tromethamine buffer[24], and the ASL pH of non-CF pigs[3] is about 7.25. Administering 60 μl of 1 mg ml^{-1} AmBisome solution through a tracheal window to 1 cm^2 of airway increased ASL pH in *CFTR*$^{-/-}$ pigs (Fig. 3d).

Thus, small-molecule ion channels can permeabilize the apical membrane of CF airway epithelia to HCO_3^- and restore ASL pH, viscosity and antibacterial activity, key components of airway host defences. CFTR selectively conducts anions, whereas the AmB channel conducts both monovalent anions and cations. AmB is therefore an imperfect substitute for CFTR. However, the mechanisms that create an electrochemical driving force for anion secretion establish a setting in which an unselective channel is sufficient to support anion secretion, the fundamental defect in CF airway epithelia. Other mechanisms may also contribute to AmB-mediated increase in transepithelial HCO_3^- transport, such as the coupling of AmB-mediated Cl^- secretion to HCO_3^- secretion by anion exchangers (for example, SLC26A4) and other apical protein anion channels (for example, SLC26A9)[28]. These findings reveal a CFTR-independent and thus genotype-independent approach for treating people with CF, including those with nonsense

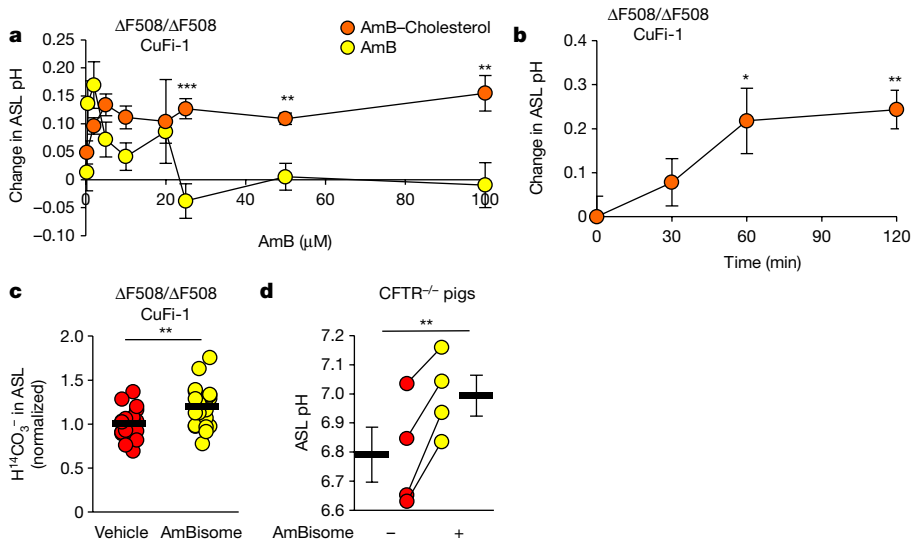

Fig. 3 | AmBisome increased ASL pH in cultured CF airway epithelia and in *CFTR*$^{-/-}$ pigs. a, Concentration-dependent effect of a preformed AmB–cholesterol complex compared to the effect of AmB on ASL pH (0 μM, $n = 37$; 0.25 μM, $n = 15$; 0.5, 50, 100 μM, $n = 9$; 2 μM, $n = 28$; 5, 10 μM, $n = 16$; 20, 25 μM, $n = 12$) in CuFi-1 (ΔF508/ΔF508) epithelia. **b**, **c**, The effect of AmBisome compared to vehicle on ASL pH in CuFi-1 epithelia as a function of time (**b**; $n = 9$) and $H^{14}CO_3^-$ secretion after 2 h (**c**; $n = 20$). **d**, Effect of AmBisome treatment on ASL pH of *CFTR*$^{-/-}$ pigs compared to baseline ($n = 4$). n is the number of biologically independent samples from at least three independent experiments with similar results. Data are mean ± s.e.m. **a**–**c**, two-sided unpaired Student's t-test (Welch's correction used for **a**: 2, 5, 20 μM and **b**: 60 min). **d**, Lines indicate measurements performed on the same pig before and after AmBisome; paired Student's t-test. $^*P \leq 0.05$; $^{**}P \leq 0.01$; $^{***}P \leq 0.001$. P values are shown in the Source Data.

and premature termination codons that produce little or no CFTR. Because this mechanism is independent of CFTR activity, there is also potential for additive effects with CFTR modulators[4,23]. Moreover, AmB is already a clinically approved drug that might benefit people with CF, and the AmBisome formulation can be safely delivered to the lungs to treat pulmonary fungal infections without producing significant systemic exposure[27,29–40].

Online content

Any methods, additional references, Nature Research reporting summaries, source data, statements of data availability and associated accession codes are available at https://doi.org/10.1038/s41586-019-1018-5.

Received: 26 July 2018; Accepted: 11 February 2019;
Published online 13 March 2019.

1. Ratjen, F. et al. Cystic fibrosis. *Nat. Rev. Dis. Primers* **1**, 15010 (2015).
2. Quinton, P. M. The neglected ion: HCO_3^-. *Nat. Med.* **7**, 292–293 (2001).
3. Shah, V. S. et al. Airway acidification initiates host defense abnormalities in cystic fibrosis mice. *Science* **351**, 503–507 (2016).
4. Ramsey, B. W. et al. A CFTR potentiator in patients with cystic fibrosis and the G551D mutation. *N. Engl. J. Med.* **365**, 1663–1672 (2011).
5. Wainwright, C. E. et al. Lumacaftor–ivacaftor in patients with cystic fibrosis homozygous for Phe508del CFTR. *N. Engl. J. Med.* **373**, 220–231 (2015).
6. Oliver, K. E., Han, S. T., Sorscher, E. J. & Cutting, G. R. Transformative therapies for rare CFTR missense alleles. *Curr. Opin. Pharmacol.* **34**, 76–82 (2017).
7. El-Etri, M. & Cuppoletti, J. Metalloporphyrin chloride ionophores: induction of increased anion permeability in lung epithelial cells. *Am. J. Physiol.* **270**, L386–L392 (1996).
8. Jiang, C. et al. Partial correction of defective Cl^- secretion in cystic fibrosis epithelial cells by an analog of squalamine. *Am. J. Physiol. Lung Cell. Mol. Physiol.* **281**, L1164–L1172 (2001).
9. Koulov, A. V. et al. Chloride transport across vesicle and cell membranes by steroid-based receptors. *Angew. Chem. Int. Ed.* **42**, 4931–4933 (2003).
10. Shen, B., Li, X., Wang, F., Yao, X. & Yang, D. A synthetic chloride channel restores chloride conductance in human cystic fibrosis epithelial cells. *PLoS ONE* **7**, e34694 (2012).
11. Poulsen, J. H., Fischer, H., Illek, B. & Machen, T. E. Bicarbonate conductance and pH regulatory capability of cystic fibrosis transmembrane conductance regulator. *Proc. Natl Acad. Sci. USA* **91**, 5340–5344 (1994).
12. Chang, E. H. et al. Medical reversal of chronic sinusitis in a cystic fibrosis patient with ivacaftor. *Int. Forum Allergy Rhinol.* **5**, 178–181 (2015).
13. Garland, A. L. et al. Molecular basis for pH-dependent mucosal dehydration in cystic fibrosis airways. *Proc. Natl Acad. Sci. USA* **110**, 15973–15978 (2013).
14. Garnett, J. P. et al. Hyperglycaemia and *Pseudomonas aeruginosa* acidify cystic fibrosis airway surface liquid by elevating epithelial monocarboxylate transporter 2 dependent lactate–H^+ secretion. *Sci. Rep.* **6**, 37955 (2016).
15. Farha, M. A., French, S., Stokes, J. M. & Brown, E. D. Bicarbonate alters bacterial susceptibility to antibiotics by targeting the proton motive force. *ACS Infect. Dis.* **4**, 382–390 (2018).
16. Peckham, D., Holland, E., Range, S. & Knox, A. J. Na^+/K^+ ATPase in lower airway epithelium from cystic fibrosis and non-cystic-fibrosis lung. *Biochem. Biophys. Res. Commun.* **232**, 464–468 (1997).
17. Widdicombe, J. H., Welsh, M. J. & Finkbeiner, W. E. Cystic fibrosis decreases the apical membrane chloride permeability of monolayers cultured from cells of tracheal epithelium. *Proc. Natl Acad. Sci. USA* **82**, 6167–6171 (1985).
18. Grillo, A. S. et al. Restored iron transport by a small molecule promotes absorption and hemoglobinization in animals. *Science* **356**, 608–616 (2017).
19. Ermishkin, L. N., Kasumov, K. M. & Potseluyev, V. M. Properties of amphotericin B channels in a lipid bilayer. *Biochim. Biophys. Acta* **470**, 357–367 (1977).
20. Gray, K. C. et al. Amphotericin primarily kills yeast by simply binding ergosterol. *Proc. Natl Acad. Sci. USA* **109**, 2234–2239 (2012).
21. Anderson, T. M. et al. Amphotericin forms an extramembranous and fungicidal sterol sponge. *Nat. Chem. Biol.* **10**, 400–406 (2014).
22. Cioffi, A. G., Hou, J., Grillo, A. S., Diaz, K. A. & Burke, M. D. Restored physiology in protein-deficient yeast by a small molecule channel. *J. Am. Chem. Soc.* **137**, 10096–10099 (2015).
23. Van Goor, F. et al. Rescue of CF airway epithelial cell function in vitro by a CFTR potentiator, VX-770. *Proc. Natl Acad. Sci. USA* **106**, 18825–18830 (2009).
24. Abou Alaiwa, M. H. et al. Repurposing tromethamine as inhaled therapy to treat CF airway disease. *JCI Insight* **1**, e87535 (2016).
25. Wallace, D. P. et al. A synthetic channel-forming peptide induces Cl^- secretion: modulation by Ca^{2+}-dependent K^+ channels. *Biochim. Biophys. Acta* **1464**, 69–82 (2000).
26. Derichs, N., Jin, B.-J., Song, Y., Finkbeiner, W. E. & Verkman, A. S. Hyperviscous airway periciliary and mucous liquid layers in cystic fibrosis measured by confocal fluorescence photobleaching. *FASEB J.* **25**, 2325–2332 (2011).
27. Monforte, V. et al. Nebulized liposomal amphotericin B prophylaxis for *Aspergillus* infection in lung transplantation: pharmacokinetics and safety. *J. Heart Lung Transplant.* **28**, 170–175 (2009).
28. Saint-Criq, V. & Gray, M. A. Role of CFTR in epithelial physiology. *Cell. Mol. Life Sci.* **74**, 93–115 (2017).
29. Ringden, O. et al. Efficacy of amphotericin B encapsulated in liposomes (AmBisome) in the treatment of invasive fungal infections in immunocompromised patients. *J. Antimicrob. Chemother.* **28**, 73–82 (1991).
30. Palmer, S. M. et al. Safety of aerosolized amphotericin B lipid complex in lung transplant recipients. *Transplantation* **72**, 545–548 (2001).
31. Drew, R. et al. Comparative safety of amphotericin B lipid complex and amphotericin B deoxycholate as aerosolized antifungal prophylaxis in lung-transplant recipients. *Transplantation* **77**, 232–237 (2004).
32. Perfect, J. R., Dodds Ashley, E. & Drew, R. Design of aerosolized amphotericin B formulations for prophylaxis trials among lung transplant recipients. *Clin. Infect. Dis.* **39**, S207–S210 (2004).
33. Lowry, C. M. et al. Safety of aerosolized liposomal versus deoxycholate amphotericin B formulations for prevention of invasive fungal infections following lung transplantation: a retrospective study. *Transpl. Infect. Dis.* **9**, 121–125 (2007).
34. Castagnola, E. et al. Nebulized liposomal amphotericin B and combined systemic antifungal therapy for the treatment of severe pulmonary aspergillosis after allogeneic hematopoietic stem cell transplant for a fatal mitochondrial disorder. *J. Chemother.* **19**, 339–342 (2013).
35. Slobbe, L., Boersma, E. & Rijnders, B. J. A. Tolerability of prophylactic aerosolized liposomal amphotericin-B and impact on pulmonary function: data from a randomized placebo-controlled trial. *Pulm. Pharmacol. Ther.* **21**, 855–859 (2008).
36. Rijnders, B. J. A. et al. Aerosolized liposomal amphotericin B for the prevention of invasive pulmonary aspergillosis during prolonged neutropenia: a randomized, placebo-controlled trial. *Clin. Infect. Dis.* **46**, 1401–1408 (2008).
37. Monforte, V. et al. Feasibility, tolerability, and outcomes of nebulized liposomal amphotericin B for *Aspergillus* infection prevention in lung transplantation. *J. Heart Lung Transplant.* **29**, 523–530 (2010).
38. Hullard-Pulstinger, A., Holler, E., Hahn, J., Andreesen, R. & Krause, S. W. Prophylactic application of nebulized liposomal amphotericin B in hematologic patients with neutropenia. *Onkologie* **34**, 254–258 (2011).
39. Monforte, V. et al. Prophylaxis with nebulized liposomal amphotericin B for *Aspergillus* infection in lung transplant patients does not cause changes in the lipid content of pulmonary surfactant. *J. Heart Lung Transplant.* **32**, 313–319 (2013).
40. Stone, N. R. H., Bicanic, T., Salim, R. & Hope, W. Liposomal amphotericin B (AmBisome®): a review of the pharmacokinetics, pharmacodynamics, clinical experience and future directions. *Drugs* **76**, 485–500 (2016).

Acknowledgements We acknowledge M. Sivaguru at the Carl R. Woese Institute for Genomic Biology for assistance with confocal microscopy, S. E. Denmark and C. Delaney for assistance with rapid injection NMR and D. J. Blair for helpful discussions. Support was provided by NIH (5R35GM118185 to M.D.B. and HL091842 to M.J.W.), and by Emily's Entourage. M.J.W. is an HHMI Investigator. K.A.M. is a Medical Scholars Fellow.

Author contributions K.A.M., R.S.C., B.R.K., M.J.W. and M.D.B. designed experiments and interpreted data. K.A.M., R.S.C., M.J.W. and M.D.B. wrote the manuscript. K.A.M., R.S.C. and P.N.D. cultured epithelia and performed Ussing chamber experiments. P.H.K. cultured primary epithelia. R.S.C. measured ion efflux, ASL ion concentrations and $H^{14}CO_3^-$ transport. K.A.M. measured ASL pH, R_t and LDH. K.A.M. and R.S.C. performed pH-stat titration. K.A.M. and A.G.C. measured ASL height. K.A.M. and X.X.T. measured ASL viscosity. K.A.M. and V.S.S. measured ASL antibacterial activity. K.A.M., R.S.C. and B.R.K. measured ASL pH in $CFTR^{-/-}$ pigs. A.S.G. synthesized compounds. L.Z. assisted NMR studies.

Competing interests K.A.M., A.G.C., A.S.G., M.J.W. and M.D.B. are inventors on patent applications PCT/US15/58806, PCT/US18/55435 and/or PCT/US2017/26806, submitted by UIUC, which cover use of AmB and AmB–cholesterol to treat CF.

Additional information
Extended data is available for this paper at https://doi.org/10.1038/s41586-019-1018-5.
Supplementary information is available for this paper at https://doi.org/10.1038/s41586-019-1018-5.
Reprints and permissions information is available at http://www.nature.com/reprints.
Correspondence and requests for materials should be addressed to M.D.B.
Publisher's note: Springer Nature remains neutral with regard to jurisdictional claims in published maps and institutional affiliations.

METHODS

Cell lines and growth conditions. NuLi, CuFi-1 and CuFi-4 cells[41] (Welsh Laboratory, University of Iowa) were first grown from cryostock on Thermo Scientific BioLite Cell Culture Treated 75 cm^2 flasks, seeded at 1.5×10^4 cells per cm^2, 1×10^3 cells per cm^2, and 1×10^4 cells per cm^2, respectively. These flasks were previously coated with 3 ml 60 μg/ml human placental collagen type IV (Sigma-Aldrich) for a minimum of 18 h at room temperature, rinsed twice with PBS, and then dried before seeding. The cells were cultured with 12 ml Bronchial Epithelial Cell Growth Medium (BEGM) BulletKit (Lonza CC-3170), which includes the basal medium and eight SingleQuots of supplements (bovine pituitary extract (BPE), 2 ml; hydrocortisone, 0.5 ml; hEGF, 0.5 ml; adrenaline, 0.5 ml; transferrin, 0.5 ml; insulin, 0.5 ml; retinoic acid, 0.5 ml; triiodothyronine, 0.5 ml). The gentamycin–AmB aliquot was discarded and the medium was instead supplemented with 50 μg/ml penicillin–streptomycin (Corning Cellgro), 50 μg/ml gentamycin (Sigma-Aldrich G1397), and 2 μg/ml fluconazole (Sigma-Aldrich). The original CF transplant donors were genotyped by Integrated Genetics. Cell lines were secondarily confirmed by the ATCC repository to have the correct genotype and were free of mycoplasma contamination. MycoAlert Mycoplasma detection kit (Lonza LT07-418) was used to detect any RNA transcripts common to a broad spectrum of mycoplasma. Cell lines were confirmed to be mycoplasma-free.

Cells were grown to 90% confluence at 37 °C in 5% CO_2, changing medium every two days, and then trypsinized with 4 ml 0.25% trypsin containing 1 mM EDTA (Gibco 25200-056). Trypsin was inactivated with 10 ml HEPES-buffered saline solution (Lonza CC-5024) with 1% bovine calf serum. Cells were spun down in an Eppendorf Centrifuge 5430R at 1,500 r.p.m. for 5 min and resuspended in BEGM medium for passaging.

For culturing on membrane supports for differentiation, cells were resuspended after centrifugation in Ultroser G medium. This comprised 1:1 DMEM:Ham's F-12, supplemented with 2% v/v Ultroser G (Crescent Chemical). The membrane supports used were Millicell 0.4-μm PCF inserts (0.6 cm^2) (Millipore PIHP01250) for Ussing chamber studies of candidate ionophores, Falcon permeable support for six-well plate with 0.4-μm transparent PET membranes (4.67 cm^2) (Fisher 08-771) in six-well companion plates (Fisher 08-771-24) for pH-stat studies, and the Corning Costar 0.4-μm 24-well plate Transwell clear polyester membrane inserts (0.33 cm^2) (Corning 3470) for all other studies. These membranes were coated with collagen in the same manner as the flasks detailed above. The Millicell inserts were seeded with 200,000 cells each, the Falcon inserts were seeded with 500,000 cells each, and the Transwell inserts were seeded with 115,000 cells each. These membranes were allowed to mature at an air–liquid interface for a minimum of 14 days to reach full differentiation as previously described[41,42], with the Ultroser G medium changed every other day. After maturation, medium was changed every seven days. For covariate control, membranes used in experiments were as close in age and maturation as possible.

Primary cultures of airway epithelia. Airway epithelial cells were obtained from human trachea and bronchi of CF and non-CF specimens obtained from the Iowa Donor Network, either as post-mortem specimens or from tissue deemed not fit for transplant. All of the corresponding genotypes are indicated in the manuscript (see Extended Data Fig. 5). All samples were deidentified in the Cell Culture Core Repository and patient identification information was not provided to the researchers doing the experiments. Patients were not recruited. Studies were approved by the University of Iowa Institutional Review Board. We have complied with all relevant ethical regulations and informed consent was obtained from all participants. After pronase enzymatic digestion, cells were seeded onto collagen-coated semi-permeable membranes (0.33–1.12 cm^2, Corning 3470 polyester, 3460 polyester or 3413 polycarbonate) and grown at an air–liquid interface using previously described methods[42]. Airway epithelial cell cultures were analysed after they had differentiated and at least 14 days after seeding.

Statistics. No data were excluded. All data are mean ± s.e.m. D'Agostino–Pearson normality test was used to confirm normal distribution of data. Statistical analysis represents *P* values obtained from one-way ANOVA or two-sided unpaired or paired Student's *t*-test where necessary. In cases where variance was not homogenous between comparison groups, a parametric *t*-test with Welch's correction was performed to account for differences in variance. NS, not significant. $*P < 0.05$, $**P \leq 0.01$, $***P \leq 0.001$ and $****P \leq 0.0001$ unless otherwise noted. On the basis of pilot experiments, we chose sample sizes that adequately power each experiment to detect a difference in outcomes between groups. Epithelial samples were manually assigned at random into control and experimental groups for each experiment. Animals served as their own controls. The investigators were not blinded to allocation during experiments and outcome assessment.

Studies of Na^+, K^+, Cl^- and $H^{13}CO_3^-$ efflux from POPC liposomes. POPC was obtained as a 25 mg/ml solution in $CHCl_3$ from Avanti Polar Lipids (850457C). The solution was stored at −20 °C under an atmosphere of dry argon and used within three months. Cholesterol (Sigma-Aldrich C8667) was purified by recrystallization from ethanol. $NaH^{13}CO_3$ was obtained as a white solid from Sigma-Aldrich (372382). Na^+, K^+ and Cl^- measurements were obtained using a Denver Instruments Model 225 pH meter equipped with the appropriate ion-selective probe inside a Faraday cage. Na^+-selective measurements were obtained using an Orion micro sodium electrode (Thermo 9811BN). K^+-selective measurements were obtained with an Orion Potassium Sure-Flow Combination Electrode with Waterproof BNC connector (Thermo 9719BNWP). Cl^--selective measurements were obtained using an Orion combination Cl^- electrode (Thermo 9617BNWP). For Na^+-efflux experiments, measurements were made on 1.5-ml solutions that were magnetically stirred in 7-ml vials incubated at 23 °C. For Cl^-- and K^+-efflux experiments, measurements were made on 4-ml solutions that were magnetically stirred in 20-ml vials incubated at 23 °C. For Na^+-, K^+- and Cl^--efflux experiments, the concentration of each ion was sampled every 10 s throughout the course of the efflux experiments. ^{13}C NMR spectra for HCO_3^- efflux experiments were acquired on a Bruker Avance III HD 500-MHz NMR spectrometer equipped with a 5-mm BBFO CryoProbe (Extended Data Fig. 1a–e), a Varian Inova 600 MHz NMR spectrometer with a Varian 10-mm broadband probe (Extended Data Fig. 1i), and a Varian Inova 600-MHz NMR spectrometer with a Varian 5-mm broadband autox probe (Extended Data Fig. 6a). The instrument was locked on D_2O. The inverse-gated ^{13}C spectra were collected.

The efflux data from each run were normalized to the percentage of total ion release from 0 to 100%. For HCO_3^--efflux experiments, after lysis of the liposome suspension, the integration of the signal corresponding to extravesicular HCO_3^- relative to the integration of the ^{13}C-glucose standard was scaled to correspond to 100% efflux. For each experimental run with AmB addition, the signal corresponding to extravesicular HCO_3^- was integrated relative to the ^{13}C internal standard for each free induction decay (FID). The scaling factor *S* was calculated for each experiment using the following relationship:

$$\left[\frac{[\mathrm{Ion}]_{\mathrm{final}}}{[\mathrm{Ion}]_{\mathrm{initial}}} - 1\right] \times S = 100$$

Each data point was then multiplied by *S* before plotting as a function of time.

Liposome preparation. Before preparing a lipid film, the lipid solution was warmed to ambient temperature to prevent condensation from contaminating the solution and degrading the lipid film. In brief, 42 mg of solid cholesterol was added to a 20-ml scintillation vial (Fisher Scientific), followed by 14 ml POPC solution. The solvent was removed with a gentle stream of nitrogen, and the resulting lipid film was stored under high vacuum for a minimum of 12 h before use. For Na^+-efflux experiments, the film was rehydrated with 2 ml 250 mM $NaHCO_3$, 40 mM HEPES buffer, pH 7.5 and vortexed vigorously for approximately 3 min to form a suspension of multilamellar vesicles (MLVs). For K^+-efflux experiments, the film was rehydrated with 2 ml 250 mM $KHCO_3$, 40 mM HEPES buffer, pH 7.5. For Cl^--efflux experiments, the film was rehydrated with 2 ml 250 mM NaCl, 40 mM HEPES buffer, pH 7.5. For HCO_3^--efflux experiments, the film was rehydrated with 2 ml 250 mM $NaH^{13}CO_3$, 40 mM HEPES buffer, pH 7.5 (D_2O). To obtain a sufficient quantity of large unilamellar vesicles (LUVs), at least two independent lipid-film preparations were pooled together for the subsequent formation of LUVs. The lipid suspension was then subjected to 15 freeze–thaw cycles, where the suspension was alternatingly allowed to freeze in a liquid nitrogen bath, followed by thawing in a 50 °C water bath. The resulting lipid suspension was pulled into a Hamilton 1-ml gas-tight syringe and the syringe was placed in an Avanti Polar Lipids Mini-Extruder (610000). The lipid solution was then passed through a 5-μm pore Whatman Nuclepore hydrophilic polycarbonate filter (VWR 28158-067) 35 times, the newly formed LUV suspension was collected in the syringe that did not contain the original suspension of MLVs to prevent the carryover of MLVs into the LUV solution. To obtain a sufficient quantity of LUVs, at least four independent 1-ml preparations were pooled together for the dialysis and subsequent efflux experiments. The newly formed LUVs were dialysed using Thermo Scientific Slide-A-Lyzer G2 dialysis cassettes (3 ml, 3,500 MWCO, 87723). Unless otherwise described, the LUV suspension was dialysed three times against 600 ml 62.5 mM $MgSO_4$, 40 mM HEPES buffer, pH 7.3. The first two dialyses were 2 h long, while the final dialysis was performed overnight.

Determination of total phosphorus was adapted from a previous report[43]. The LUV suspension was diluted 40-fold with 62.5 mM $MgSO_4$ in 40 mM HEPES buffer pH 7.3. Three 10-μl samples of the diluted LUV suspension were added to three separate 7-ml vials. Subsequently, the solvent was removed with a stream of N_2. H_2SO_4 (8.9 M, 450 μl) was added to each dried LUV film, including to a fourth vial containing no lipids that was used as a blank. The four samples were incubated open to ambient atmosphere in a 225 °C aluminium heating block for 25 min and then moved to 23 °C and allowed to cool for 5 min. After cooling, 150 μl 30% w/v aqueous hydrogen peroxide was added to each sample, and the vials were returned to the 225 °C heating block for 30 min. The samples were then moved to 23 °C and allowed to cool for 5 min before the addition of 3.9 ml water. Then, 500 μl 2.5% w/v ammonium molybdate was added to each vial, and the resulting mixtures were

vortexed briefly and vigorously five times. Subsequently, 500 μl 10% w/v ascorbic acid was added to each vial, and the resulting mixtures were vortexed briefly and vigorously five times. The vials were enclosed with a PTFE-lined cap and then placed in a 100 °C aluminium heating block for 7 min. The samples were moved to 23 °C and allowed to cool for approximately 15 min before analysis by UV/vis spectroscopy. Total phosphorus was determined by observing the absorbance at 820 nm and comparing this value to a standard curve obtained using this method with standard solutions with known concentrations of phosphorus.

Efflux from LUVs. *^{13}C NMR studies of $H^{13}CO_3^-$ efflux from POPC liposomes.* Cholesterol-containing POPC liposomes were prepared as described above. The LUV suspension was dialysed 10 times against 300 ml 87 mM Na_2SO_4 in 40 mM HEPES buffer pH 7.3 (H_2O) with stirring. The first dialysis was 4 h long, and the subsequent nine dialyses were performed for 1 h. Determination of phosphorous content was performed as described above.

The pooled LUV suspension was diluted to 70 mM lipid with 87 mM Na_2SO_4, 40 mM HEPES buffer, pH 7.3 (D_2O), and 0.025% (w/v) ^{13}C D-glucose (1-^{13}C) (Sigma-Aldrich 297046) was added as an internal standard. ^{13}C NMR spectra were acquired on a Bruker Avance III HD 500 MHz NMR spectrometer equipped with a 5-mm BBFO CryoProbe. The ^{13}C frequency was set to 125.83 MHz, and spectral width was 31,512 Hz. The instrument was locked on D_2O. Experimental conditions were: acquisition time, 0.93 s; 30° pulse width, 3.3 μs; relaxation delay, 0.2 s; number of scans, 256; temperature, 23 °C.

For each experiment, 1.4 μl vehicle, AmB, or C35deOAmB (17.5 μM final concentration, 100× stock solution in DMSO) was added to 140 μl liposome suspension. The liposome suspension was immediately transferred to a New Era (NE-H5/4) micro NMR sample tube (3 mm lower/5 mm upper), and eight consecutive FIDs were obtained as described above. For experimental runs with $MnCl_2$, 5 μl 50 mM $MnCl_2$ solution was added after the addition of AmB. To effect complete ion release, 10 μl 30% (v/v) solution of Triton X-100 (Sigma-Aldrich X100) was added to the liposome suspension before data acquisition[44–47].

Na^+, K^+, and Cl^- efflux from POPC liposomes. For Na^+-, K^+- and Cl^--efflux experiments, the pooled LUV suspension was diluted to 70 mM lipid with 62.5 mM $MgSO_4$, 40 mM HEPES buffer, pH 7.3. The LUV suspension (1.5 ml for Na^+ and 4 ml for Cl^- and K^+) was added to either a 7-ml (Na^+) or 20-ml vial (Cl^- and K^+) and magnetically stirred. The appropriate probe was inserted, and data were collected for 1 min before addition of AmB. For Na^+-efflux experiments, 15 μl of either vehicle or AmB (70 μM final concentration, 100× stock solution in DMSO) was added to 1.5 ml LUV suspension, and data were collected for 10 min. To effect complete ion release, 15 μl 30% (v/v) Triton X-100 was added, and data were collected for an additional 5 min. For Cl^-- and K^+-efflux experiments, 40 μl of either vehicle or AmB (70 μM final concentration, 100× stock solution in DMSO) was added to 4 ml LUV suspension, and data were collected for 10 min. To effect complete ion release, 40 μl 30% v/v solution of Triton X-100 was added, and data were collected for an additional 5 min.

$H^{13}CO_3^-$ efflux from POPC liposomes with rapid-injection NMR. Cholesterol-containing POPC liposomes were prepared as described above. The LUV suspension was dialysed three times against 600 ml 62.5 mM $MgSO_4$ in 40 mM HEPES buffer pH 7.3 (9:1 H_2O:D_2O) with stirring. The first two dialyses were 2 h long, whereas the final dialysis was performed overnight. Determination of phosphorous content was performed as described above. $H^{13}CO_3^-$ efflux was measured using rapid injection NMR[48,49]. ^{13}C NMR spectra were acquired using a Varian Inova 600MHz NMR spectrometer with a Varian 10-mm broadband probe. The ^{13}C frequency was set to 150.83 MHz, and spectral width was 37,037 Hz. Experimental conditions were: acquisition time, 0.50 s; 45° pulse width, 14 μs; relaxation delay, 1.5 s; number of scans, 1; temperature, 23 °C. LUV suspension (2.5 ml) was added to an oven-dried 10-mm NMR tube (New Era Enterprises, NE-H10-7). The uncapped tube was placed into the probe of the NMR spectrometer. AmB (70 μM, 100× stock in DMSO) was injected at a rate of 500 μl per second. The injector was used to mix the sample followed by data collection. The efflux of HCO_3^- was monitored by ^{13}C NMR by collecting 300 consecutive spectra over the course of 10 min after addition. To effect complete ion release, 80 μl of a 10% (v/v) solution of Triton X-100 was added to the liposome suspension before data acquisition[44–47].

Studies of H^+ efflux from POPC liposomes. H^+ efflux from POPC–10% cholesterol liposomes was determined as previously described[50].

$H^{13}CO_3^-$ efflux from POPC liposomes with AmBisome and AmB:cholesterol. The LUV suspension was dialysed three times against 600 ml 62.5 mM $MgSO_4$ in 40 mM HEPES buffer pH 7.3 (H_2O) with stirring. The first two dialyses were 2 h long, whereas the final dialysis was performed overnight. Determination of phosphorous content was performed as described above.

The pooled LUV solution was diluted to 100 mM lipid with 62.5 mM $MgSO_4$, 40 mM HEPES buffer, pH 7.3 (D_2O), and 0.025% (w/v) ^{13}C D-glucose (1-^{13}C) was added as an internal standard. ^{13}C NMR spectra were acquired on a Varian Inova 600MHz NMR spectrometer with a Varian 5-mm broadband autox probe. The ^{13}C frequency was set to 125.83 MHz, and spectral width was 31,512 Hz. The instrument was locked on D_2O. Experimental conditions were: acquisition time, 0.93 s; 30° pulse width, 3.3 μs; relaxation delay, 0.2 s; number of scans, 256; temperature, 23 °C.

For each experiment, 5 μl DMSO or sterile water vehicle, AmBisome in sterile water, or AmB:cholesterol in DMSO (100 μM final AmB concentration, 100× stock solution) was added to 500 μl liposome suspension in an oven-dried New Era 5-mm NMR sample tube. Twelve consecutive FIDs were obtained as described above. To effect complete ion release, 40 μl 10% (v/v) Triton X-100 solution was added to the liposome suspension before data acquisition[44–47].

Measurement of ASL pH in cell line and primary cultures of airway epithelia. Small-diameter NuLi, CuFi and primary cultured epithelia were used for this experiment (0.33 cm^2). The ratiometric pH indicator SNARF-conjugated dextran (Molecular Probes) was used to measure ASL pH. SNARF powder was suspended via sonication in perfluorocarbon-72 (Sigma-Aldrich FC-72) and distributed onto the apical surface. ASL pH was measured 2 h later[3,12,51]. SNARF was excited at 488 nm and emission was recorded at 580 nm and 640 nm using a Zeiss LSM 800 microscope at ×40 water immersion for cell line cultures and a Zeiss LSM 510 microscope for primary cultures. To generate a standard curve for pH determination, SNARF was dissolved in colorless pH standards and fluorescence ratios were converted to pH.

Agents tested in this assay were first lyophilized into powder and then suspended in the appropriate volume of perfluorocarbon, which were sonicated for 1 min to aid suspension. AmBisome should not be sonicated; instead, the fine powder was suspended by vortexing. Subsequently, 20 μl of this suspension was administered onto the surface of cultured airway epithelia (0.33 cm^2) at the following approximate concentrations in suspension: AmB, 0.25–100 μM; AmB–cholesterol complex, 0.5—100 μM; C35deOAmB[20], 2 μM; 10 μM forskolin/10 μM ivacaftor[12]; AmBisome 6–2,450 μg/ml.

In all experiments, ASL pH of compound-treated epithelia was measured and compared to the results from vehicle-treated epithelia.

For apical AmB administration, cultured airway epithelia were incubated for between 30 min and 48 h at 37 °C before measurement of ASL pH. For AmB–cholesterol complex and C35deOAmB administration, cultured airway epithelia were incubated for 48 h at 37 °C before measurement of ASL pH. For 10 μM ivacaftor/10 μM forskolin administration, cultured airway epithelia were incubated for 2 h at 37 °C before measurement of ASL pH[12]. For basolateral AmB administration, a 2 mM stock of AmB in DMSO was diluted 1,000-fold to a final concentration of 2 μM in USG medium. The basolateral medium of cultured airway epithelia was replaced with the AmB-containing USG medium and incubated for 48 h at 37 °C before measurement of ASL pH.

Specific conditions for experiments in Figs. 1–3 not otherwise described in legends: Fig. 1a, ivacaftor/forskolin (10 μM, 2 h); apical AmB (2 μM, 48 h); Fig. 1c, ivacaftor/forskolin (10 μM, 2 h), AmB (2 μM, 48 h), C35deOAmB (2 μM, 48 h), basolateral addition of AmB (2 μM, 48 h); Fig. 1e, AmB (2 μM, 48 h); Fig. 1f, AmB (2 μM); Fig. 2a, AmB (2 μM, 48 h); Fig. 2b, AmB (2 μM); Fig. 3a, AmB (48 h); and Fig. 3b, AmBisome (1 mg/ml).

pH-stat titration of NuLi and CuFi monolayers. Large-diameter NuLi and CuFi-1 cultured epithelia were used for this experiment (4.67 cm^2). These cultures were mounted in a dual-channel Ussing chamber (Warner U2500) using the culture cup insert for Transwell adaptor, 24 mm (U9924T-24). The membranes were bathed at 37 °C on the apical side with a buffer-free solution (140 mM NaCl, 2 mM KCl, 2 mM $CaCl_2$, 1 mM $MgCl_2$, 15 mM dextrose, gassed with air) and on the basolateral side with either a HCO_3^- buffer (120 mM NaCl, 25 mM $NaHCO_3$, 5 mM KCl, 2 mM $CaCl_2$, 1.2 mM $MgCl_2$, 13.75 NaH_2PO_4, 5.6 mM dextrose, pH adjusted to 7.0) or a HCO_3^--free buffer (140 mM NaCl, 2 mM KCl, 2 mM $CaCl_2$, 1 mM $MgCl_2$, 10 mM HEPES, 5 mM dextrose, pH adjusted to 7.0). A microdiameter pH electrode (89231-590) and temperature probe (Radiometer Analytical T201 Temperature Sensor, E51M001) and titration burette attached to a Hach TIM856 NB pH/EP/Stat pH-STAT Titrator (R41T028) were inserted into the apical chamber. The basolateral chamber was covered with the chamber lid to prevent gas exchange. The pH electrode was then calibrated using known pH solutions (Hach, S11M002, S11M004, S11M007).

The apical pH was titrated to a target pH of 6.0 using 1 mM HCl as titrant (minimum speed 0.25 ml/min, maximum speed 0.35 ml/min)[52–55]. Acid titration was measured over 20 min to establish a baseline value for the cultured epithelia (maximum speed 2 ml/min). Both apical and basolateral bathing solutions were then removed. A stock solution of AmB in DMSO was added to a final concentration of 0.5, 1 or 5 μM in an aliquot of buffer-free solution and added to the apical chamber, and the basolateral chamber was replaced with fresh HCO_3^- or HCO_3^--free buffer. The apical pH was again titrated to a target pH of 6.0 using 1 mM HCl as titrant. Acid titration was then measured over another 20 min to evaluate AmB-mediated pH change in the apical solution.

Data were plotted as nmoles of H^+ titrated in per min, and the slope of this curve was divided by the area of the culture (4.67 cm^2) to obtain the rate of acid titration (nmoles H^+ min^{-1} cm^{-2}).

Determination of ASL Na^+, K^+, Mg^{2+} and Ca^{2+} concentrations in CuFi-1 monolayers. Small-diameter CuFi-1 cultured epithelia were used for this experiment (0.33 cm^2). In brief, 24 h before the start of the experiment, the apical side of all cultured epithelia was rinsed three times with 200 μl warm PBS to remove excess mucus. Fresh USG medium was first added to the basolateral membrane. CuFi-1 epithelia were treated with either perfluorocarbon vehicle or 2 μM AmB suspended in perfluorocarbon, and incubated at 37 °C for 48 h. Microcapillary tubes (0.1 μl capacity, Drummond Scientific NC1453214) were placed into 200-μl pipette tips (Denville Scientific P1122). Then, 48 h after AmB addition, the microcapillary tubes were gently touched around the edge of the apical membrane of each epithelial culture insert until they were completely filled with ASL via capillary action. After collecting 0.1 μl ASL, a p200 pipette was used to push the entire sample into 15 μl molecular biology grade water (Corning 46-000-CM). The sample was then quantitatively transferred to a 15-ml conical vial by washing three times with 50 μl molecular biology grade water.

Quantification of sodium, magnesium, potassium and calcium was accomplished using inductively coupled plasma mass spectrometry (ICP-MS) of acidified samples. Each sample was diluted to a final volume of 5 ml with 1.0% HNO_3 (v/v) in double-distilled water. Quantitative standards were made using mixed Na, Mg, K and Ca standards containing 100 μg/ml of each element (Inorganic Ventures), which were combined to create a 100 ng/ml mixed-element standard in 1.0% nitric acid (v/v).

ICP-MS was performed on a computer-controlled (QTEGRA software) Thermo iCapQ ICP-MS (Thermo Fisher Scientific) operating in KED mode and equipped with a ESI SC-2DX PrepFAST autosampler. Internal standard was added inline using the prepFAST system and consisted of 1 ng/ml of a mixed element solution containing Bi, In, ^{6}Li, Sc, Tb and Y (IV-ICPMS-71D from Inorganic Ventures). Online dilution was also carried out using the prepFAST system and used to generate calibration curves with 5,000, 1,000, 500, 100 and 50 ng/ml Na, Mg, K and Ca. Each sample was acquired using one survey run (ten sweeps) and three main (peak-jumping) runs (40 sweeps). The isotopes selected for analysis were ^{23}Na, ^{24}Mg, ^{39}K, ^{44}Ca, and ^{89}Y (chosen as internal standards for data interpolation and machine stability). Instrument performance was optimized daily through autotuning followed by verification via a performance report (passing manufacturer's specifications).

$H^{14}CO_3^-$ transport across NuLi and CuFi monolayers. Small-diameter NuLi and CuFi cultured epithelia were used for this experiment (0.33 cm^2). ^{14}C-labelled sodium bicarbonate was obtained as a sterile 35.7 mM aqueous solution pH 9.5 (MP Biomedicals 0117441H). All experiments were run less than two months after seeding. Fresh USG medium was added to the basolateral side before experimentation. The apical membrane was treated with 20 μl vehicle, AmB, or ivacaftor/forskolin as a suspension in perfluorocarbon, and the cultured epithelia were incubated for 48 h, 7 days, 14 days or 28 days at 37 °C in a 5% CO_2 atmosphere. After the end of the treatment period, 5 μl 1.4 mM $H^{14}CO_3^-$ stock solution in USG medium was added to the basolateral medium. The cultured epithelia were then incubated at 37 °C for 10 min. After 10 min, the apical membrane of the cultured epithelia was immediately washed with 200 μl PBS. The ASL wash and a 200 μl aliquot of the basolateral medium were diluted in scintillation cocktail (Perkin Elmer 6013199) and analysed by liquid scintillation counting[18]. The measured rate of basolateral-to-apical $H^{14}CO_3^-$ secretion was then normalized to the vehicle-treated control.

Specific conditions for experiments in Figs. 1–3 not otherwise described in legends: Fig. 1b, ivacaftor/forskolin (10 μM, 2 h), apical AmB (2 μM, 48 h); Fig. 1d, ivacaftor/forskolin (10 μM, 2 h), AmB (2 μM, 48 h), C35deOAmB (2 μM, 48 h), basolateral addition of AmB (2 μM, 48 h); Fig. 3c, AmBisome (1 mg/ml).

ASL pH and $H^{14}CO_3^-$ studies with basolateral ouabain. Small-diameter CuFi-1 cultured epithelia were used for this experiment (0.33 cm^2). All experiments were run less than two months after seeding. Fresh USG medium was added to the basolateral side before experimentation. The apical membrane was treated with 20 μl vehicle or 2 μM AmB as a suspension in perfluorocarbon, and the cultured epithelia were incubated for 47 h at 37 °C in a 5% CO_2 atmosphere. The basolateral medium was then removed and replaced with 10 mM ouabain[56] (Sigma-Aldrich O3125) dissolved in a low sodium Ringer's buffer (125 mM choline chloride, 10 mM NaCl, 14 mM $KHCO_3$, 5 mM HEPES, 2.4 mM K_2HPO_4, 0.6 mM KH_2PO_4, 1.2 mM $CaCl_2$, 1.2 mM $MgCl_2$, 5 mM dextrose, pH 7.4 with 10 N NaOH) at 37 °C. The epithelia were then incubated at 37 °C for 1 h. After 1 h, ASL pH and $H^{14}CO_3^-$ were measured as described above.

Ussing Chamber studies of NuLi and CuFi monolayers. To assess the presence of membrane-expressed CFTR, differentiated cultures of NuLi and CuFi-1 epithelia grown on Corning Costar 0.4 μm 24-well plate Transwell Clear Polyester Membrane inserts were used. NuLi and CuFi-1 epithelia were treated with 20 μl perfluorocarbon vehicle or 2 μM AmB sonicated into a suspension in perfluorocarbon. After 48 h of incubation, the epithelia were mounted in a dual-channel Ussing chamber (Warner U2500) using the culture cup insert for Transwell adaptor, 6.5 mm (Warner U9924T-06) and bathed on both the apical and basolateral sides with a HCO_3^- solution (120 mM NaCl, 25 mM $NaHCO_3$, 5 mM KCl, 2 mM $CaCl_2$, 1.2 mM $MgCl_2$, 13.75 mM NaH_2PO_4, pH 7.0) at 37 °C and gassed with compressed air. Dextrose was added to this solution immediately before experiments to a final concentration of 5.6 mM. Epithelial Na^+ channel (ENaC) and calcium-activated Cl^- channel (CaCC) were inhibited by apical addition of 100 μM amiloride and 100 μM DIDS (4,4′-disothiocyanostilbene-2,2′-disulfonic acid), respectively, to achieve a baseline for permeabilization. Forskolin (10 μM) and 100 μM 3-isobutyl-1-methylxanthine (IBMX), added apically, were used to activate CFTR, and 1 μM $CFTR_{inh}$-172 (Selleck Chemicals S7139) was used to inhibit CFTR. Each successive addition of reagent was allowed approximately 10 min to equilibrate before the addition of the next reagent[41].

Measurement of transepithelial electrical resistance. Small-diameter CuFi-1 cultured epithelia were used for this experiment (0.33 cm^2). Cultured epithelia were treated with perfluorocarbon vehicle, 2 μM AmB or 50 μM AmB administered in perfluorocarbon as previously described for 48 h, 7 days, or 28 days. Fresh USG medium (200 μl) was placed on the apical side of the epithelia. Transepithelial electrical resistance (R_t) was then measured using a Millicell ERS-2 Voltohmmeter across the apical and basolateral sides of the epithelia in a snaking pattern for two technical replicates per biological replicate.

Lactate dehydrogenase assay. Small-diameter CuFi-1 cultured epithelia were used for this experiment (0.33 cm^2). A lactate dehydrogenase (LDH) Cytotoxicity Assay Kit (Cayman Chemical) was used to determine whether AmB was toxic to CuFi-1 airway epithelia. Before treatment, medium was removed from the basolateral side of epithelia and replaced with 500 μl fresh USG medium. Cultured epithelia were then treated with perfluorocarbon vehicle, 2 μM AmB or 50 μM AmB administered in perfluorocarbon as previously described for 48 h, 7 days, or 28 days. Subsequently, 48 h before the end of each experiment time frame, basolateral medium was changed again and 20 μl 10% Triton X-100 solution was added to the apical surface to elicit maximum release. On the day of the experiment, assay reagents were prepared according to the kit instructions and 500 μl USG medium was added to three empty wells in a 24-well plate for background control. Culture inserts were removed from the wells and 250 μl LDH Reaction Solution was added to each well. The plate was then gently shaken on an orbital shaker for 30 min at 37 °C. Absorbance was read at 490 nm using a plate reader. The percentage of cytotoxicity was calculated as follows:

$$\text{Cytotoxicity}(\%) = \frac{(A_{490\text{ nm}} - A_{490\text{ nm}}^{\text{background}})}{(A_{490\text{ nm}}^{\text{max}} - A_{490\text{ nm}}^{\text{background}})}$$

where $A_{490\text{ nm}}$ is the absorbance at 490 nm, and background and max represent background and maximum values, respectively.

ASL height assay. ASL height was studied using an established fluorescent-dye-based assay[57,58]. Small-diameter NuLi and CuFi-1 cultured epithelia were used for this experiment (0.33 cm^2). In brief, 24 h before the start of the experiment, the apical side of all cultured epithelia was rinsed three times with warm PBS to remove excess mucus. NuLi epithelia were treated with perfluorocarbon vehicle or 500 μM basolateral bumetanide in DMSO vehicle applied to the medium, and CuFi epithelia were treated with 20 μl vehicle, 0.5 μM AmB or 0.5 μM C35deOAmB suspended in perfluorocarbon, with or without 500 μM basolateral bumetanide in DMSO vehicle applied to the medium and incubated for 24 h at 37 °C. For basolateral AmB administration, a 2 mM stock of AmB in DMSO was diluted 1,000-fold to a final concentration of 2 μM in USG medium. The basolateral medium of cultured airway epithelia was replaced with the AmB-containing USG medium. After 24 h, 2.5 μl 2 mg/ml 70-kDa Texas red–dextran conjugate (Molecular Probes) solution in PBS was added to the apical side of the epithelia, followed by 100 μl FC-770 to prevent evaporation. Then, the culture support was placed on top of 100 μl PBS on a 10-mm glass bottom Fluorodish for imaging (World Precision Instruments). Epithelia were imaged immediately after dye addition and again at 24 h to examine dye absorption. Three *z*-stack images per membrane were taken on an Zeiss LSM700 confocal microscope with a 40× oil-immersion objective. These images were analysed using ImageJ[59] to determine the average ASL height in the centre 1,300 pixels of each image. Images were smoothed, converted to 8-bit, and thresholded to most accurately represent the red area. The parameters for the 'analyze particles' function in ImageJ were 'particles from 1 μm^2 to infinity in size and from 0 to 100% circularity'. Height was determined by dividing the area output in pixels by the known 1,300-pixel width and converted to μm using the known scaling factor of 0.49 μm $pixel^{-1}$.

Viscosity of AmB-treated primary cultures of airway epithelia. ASL viscosity in airway epithelial cultures was determined as previously described[12,60].

Small-diameter primary cultured epithelia were used for this experiment (0.33 cm^2). The apical surface was not washed for at least two weeks before study. Cultured epithelia were treated with 2 μM AmB administered in perfluorocarbon, as previously described, for 48 h. FITC–dextran (70 kDa, Sigma-Aldrich) was then administered to the apical surface of epithelia as a dry powder 2 h before measurement of viscosity. FRAP was assayed in a humidified chamber at 37 °C using a Zeiss LSM 510 META microscope. Images were acquired until maximal recovery was reached. At least six recovery curves from different locations in each culture were acquired and averaged to obtain data for one epithelial culture. The time constant (τ_{saline}) was calculated by regression analysis from fluorescence recovery curves. Viscosity is expressed relative to the time constant of saline (τ_{ASL}/τ_{saline}).

Antibacterial activity of AmB-treated primary cultures of airway epithelia. *S. aureus*-coated gold grids were used to measure antibacterial activity of airway epithelial cultures as previously described[3,51]. Small-diameter primary cultured epithelia were used for this experiment (0.33 cm^2). Bacteria-coated gold transmission electron microscopy grids were placed onto the apical surface of airway epithelia for 1 min after 48 h of perfluorocarbon, 2 μM AmB, or 2 μM C35deOAmB treatment. As controls, bacteria-coated grids were also placed in saline or AmB in perfluorocarbon laid over saline to simulate the administration method for 1 min. After removal, bacteria on the grids were assessed for viability using Live/Dead BacLight Bacterial Viability assay (Invitrogen). Viability was determined in four to six fields to determine the percentages of dead bacteria.

Animal studies. We studied female and male newborn pigs with targeted disruption of the *CFTR* gene ($CFTR^{-/-}$), generated from mating $CFTR^{+/-}$ pigs. Pigs were obtained from Exemplar Genetics. The University of Iowa Animal Care and Use Committee approved all animal studies, and we complied with all relevant ethical regulations.

Measurement of ASL pH in *CFTR*$^{-/-}$ pigs. ASL pH was measured in pigs in vivo as previously described[24,51]. To administer AmBisome in pig trachea, pigs were initially sedated with ketamine (Ketaject, Phoenix; 20 mg/kg, intramuscular injection) and anaesthetized using propofol (Diprivan, Fresenius Kabi; 2 mg/kg, intravenous injection). The trachea was surgically exposed and accessed anteriorly, and a small anterior window was cut through the tracheal rings. To mimic physiologic conditions, data were obtained in a 100% humidified chamber at 37 °C and constant 5% CO_2.

For the first $CFTR^{-/-}$ pig, a baseline ASL pH measurement was taken for about 8 min before 60 μl 100 μg/ml AmBisome in perfluorocarbon was administered to the tracheal window. ASL pH was continually measured for 60 min. Then, 60 μl 1 mg/ml AmBisome was administered to the tracheal window and pH was continually measured for another 60 min. For the second $CFTR^{-/-}$ pig, a baseline ASL pH measurement was taken for about 8 min before 60 μl perfluorocarbon vehicle was administered to the tracheal window as an internal control. ASL pH was continually measured for another 30 min. Then, 60 μl 1 mg/ml AmBisome was administered to the tracheal window and continuous measurements were then taken for 106 min. For the third and fourth $CFTR^{-/-}$ pigs, a baseline ASL pH measurement was taken for about 10 min. Then, 60 μl 1 mg/ml AmBisome in perfluorocarbon was administered to the tracheal window and continuous measurements were taken for 120 min.

Reporting summary. Further information on research design is available in the Nature Research Reporting Summary linked to this paper.

Data availability

All data generated or analysed during this study are included in the paper and its Supplementary Information. Source Data are available in the online version of the paper for Figs. 1–3 and Extended Data Figs. 1–3, 5, 6.

41. Zabner, J. et al. Development of cystic fibrosis and noncystic fibrosis airway cell lines. *Am. J. Physiol. Lung Cell. Mol. Physiol.* **284**, L844–L854 (2003).
42. Karp, P. H. et al. An in vitro model of differentiated human airway epithelia. Methods for establishing primary cultures. *Methods Mol. Biol.* **188**, 115–137 (2002).
43. Chen, P. S., Toribara, T. Y. & Warner, H. Microdetermination of phosphorus. *Anal. Chem.* **28**, 1756–1758 (1956).
44. Andrews, N. J. et al. Structurally simple lipid bilayer transport agents for chloride and bicarbonate. *Chem. Sci.* **2**, 256–260 (2011).
45. Busschaert, N. et al. Tripodal transmembrane transporters for bicarbonate. *Chem. Commun.* **46**, 6252–6254 (2010).
46. Davis, J. T. et al. Using small molecules to facilitate exchange of bicarbonate and chloride anions across liposomal membranes. *Nat. Chem.* **1**, 138–144 (2009).
47. Busschaert, N. et al. Synthetic transporters for sulfate: a new method for the direct detection of lipid bilayer sulfate transport. *Chem. Sci.* **5**, 1118–1127 (2014).
48. Denmark, S. E., Williams, B. J., Eklov, B. M., Pham, S. M. & Beutner, G. L. Design, validation, and implementation of a rapid-injection NMR system. *J. Org. Chem.* **75**, 5558–5572 (2010).
49. Thomas, A. A. & Denmark, S. E. Pre-transmetalation intermediates in the Suzuki–Miyaura reaction revealed: the missing link. *Science* **352**, 329–332 (2016).
50. Davis, S. A. et al. C3-OH of amphotericin B plays an important role in ion conductance. *J. Am. Chem. Soc.* **137**, 15102–15104 (2015).
51. Pezzulo, A. A. et al. Reduced airway surface pH impairs bacterial killing in the porcine cystic fibrosis lung. *Nature* **487**, 109–113 (2012).
52. Cho, D. Y., Hajighasemi, M., Hwang, P. H., Illek, B. & Fischer, H. Proton secretion in freshly excised sinonasal mucosa from asthma and sinusitis patients. *Am. J. Rhinol. Allergy* **23**, e10–e13 (2009).
53. Cho, D. Y., Hwang, P. H., Illek, B. & Fischer, H. Acid and base secretion in freshly excised nasal tissue from cystic fibrosis patients with ΔF508 mutation. *Int. Forum Allergy Rhinol.* **1**, 123–127 (2011).
54. Fischer, H. & Widdicombe, J. H. Mechanisms of acid and base secretion by the airway epithelium. *J. Membr. Biol.* **211**, 139–150 (2006).
55. Fischer, H. Function of proton channels in lung epithelia. *Wiley Interdiscip. Rev. Membr. Transp. Signal.* **1**, 247–258 (2012).
56. Devor, D. C. et al. Bicarbonate and chloride secretion in Calu-3 human airway epithelial cells. *J. Gen. Physiol.* **113**, 743–760 (1999).
57. Myerburg, M. M. et al. AMPK agonists ameliorate sodium and fluid transport and inflammation in cystic fibrosis airway epithelial cells. *Am. J. Respir. Cell Mol. Biol.* **42**, 676–684 (2010).
58. Worthington, E. N. & Tarran, R. Methods for ASL measurements and mucus transport rates in cell cultures. *Methods Mol. Biol.* **742**, 77–92 (2011).
59. Schneider, C. A., Rasband, W. S. & Eliceiri, K. W. NIH Image to ImageJ: 25 years of image analysis. *Nat. Methods* **9**, 671–675 (2012).
60. Tang, X. X. et al. Acidic pH increases airway surface liquid viscosity in cystic fibrosis. *J. Clin. Invest.* **126**, 879–891 (2016).

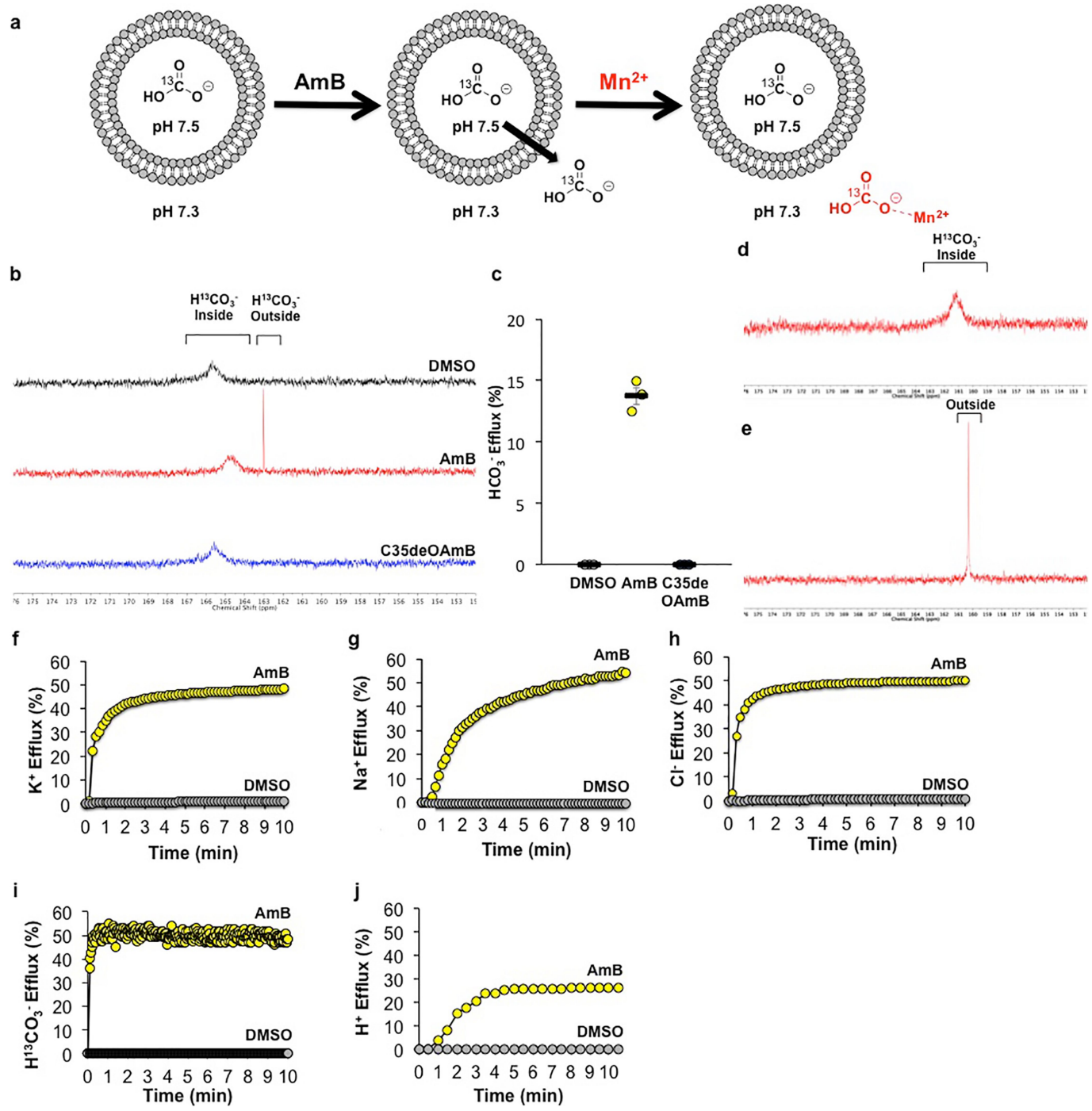

Extended Data Fig. 1 | See next page for caption.

Extended Data Fig. 1 | AmB can transport K^+, Na^+, Cl^-, H^+ and HCO_3^- across a lipid membrane. Traces indicate the percentage of maximum ion efflux after Triton X-100 addition. **a**, Schematic for the ^{13}C NMR HCO_3^- efflux experiment. **b**, ^{13}C NMR spectra of $H^{13}CO_3^-$-loaded POPC/10% cholesterol liposomes treated with AmB, C35deOAmB, or DMSO vehicle. $NaH^{13}CO_3$ was loaded inside the liposomes and the intravesicular solution was buffered to pH 7.5, whereas the extravesicular solution was buffered to pH 7.3. Owing to this pH difference, intravesicular HCO_3^- displays a more downfield chemical shift relative to extravesicular HCO_3^-. Addition of AmB (1:4,000 AmB:POPC) produces an upfield ^{13}C signal corresponding to extravesicular HCO_3^-, while the addition C35deOAmB or DMSO vehicle does not, demonstrating that AmB is able to facilitate HCO_3^- efflux. **c**, The percentage of efflux of HCO_3^- mediated by DMSO, AmB or C35deOAmB, quantified 10 min after addition to POPC liposomes ($n = 3$ biologically independent samples). Data from each run were normalized to the percentage of total ion release from 0 to 100%. After lysis of the liposome suspension, the integration of the signal corresponding to extravesicular HCO_3^- relative to the integration of a ^{13}C-glucose standard was scaled to correspond to 100% efflux. **d**, To confirm that the upfield signal corresponds to extravesicular HCO_3^-, Mn^{2+}—which binds to HCO_3^- and quenches the observed ^{13}C signal via paramagnetic relaxation enhancement—was added to the extravesicular solution. Because Mn^{2+} is impermeable to the POPC bilayer, Mn^{2+} can only affect the signal corresponding to HCO_3^- outside the liposomes. Addition of Mn^{2+} quenched the upfield signal produced with the addition of AmB but not the signal corresponding to intravesicular HCO_3^-, confirming that AmB causes efflux of HCO_3^-. **e**, To effect complete ion release, the POPC liposomes were lysed with Triton X-100 at the conclusion of the experiment. **f**, K^+ efflux from POPC/10% cholesterol liposomes after addition of AmB equivalent to 1:1,000 AmB:lipid, or DMSO vehicle. **g**, Na^+ efflux from POPC/10% cholesterol liposomes after addition of AmB equivalent to 1:1,000 AmB:lipid, or DMSO vehicle. **h**, Cl^- efflux from POPC/10% cholesterol liposomes after addition of AmB equivalent to 1:1,000 AmB:lipid, or DMSO vehicle. **i**, HCO_3^- efflux from POPC/10% cholesterol liposomes after addition of AmB equivalent to 1:1,000 AmB:lipid, or DMSO vehicle. Kinetics of efflux were measured using rapid-injection NMR to add AmB to liposomes. **j**, H^+ efflux from POPC/10% cholesterol liposomes after addition of AmB equivalent to 1:1,000 AmB:lipid, or DMSO vehicle. **b**, **d**–**j**, Panels show a representative spectrum or graph from at least three independent experiments. In all panels, measurements were taken from distinct samples. In **c**, the graph depicts mean ± s.e.m.

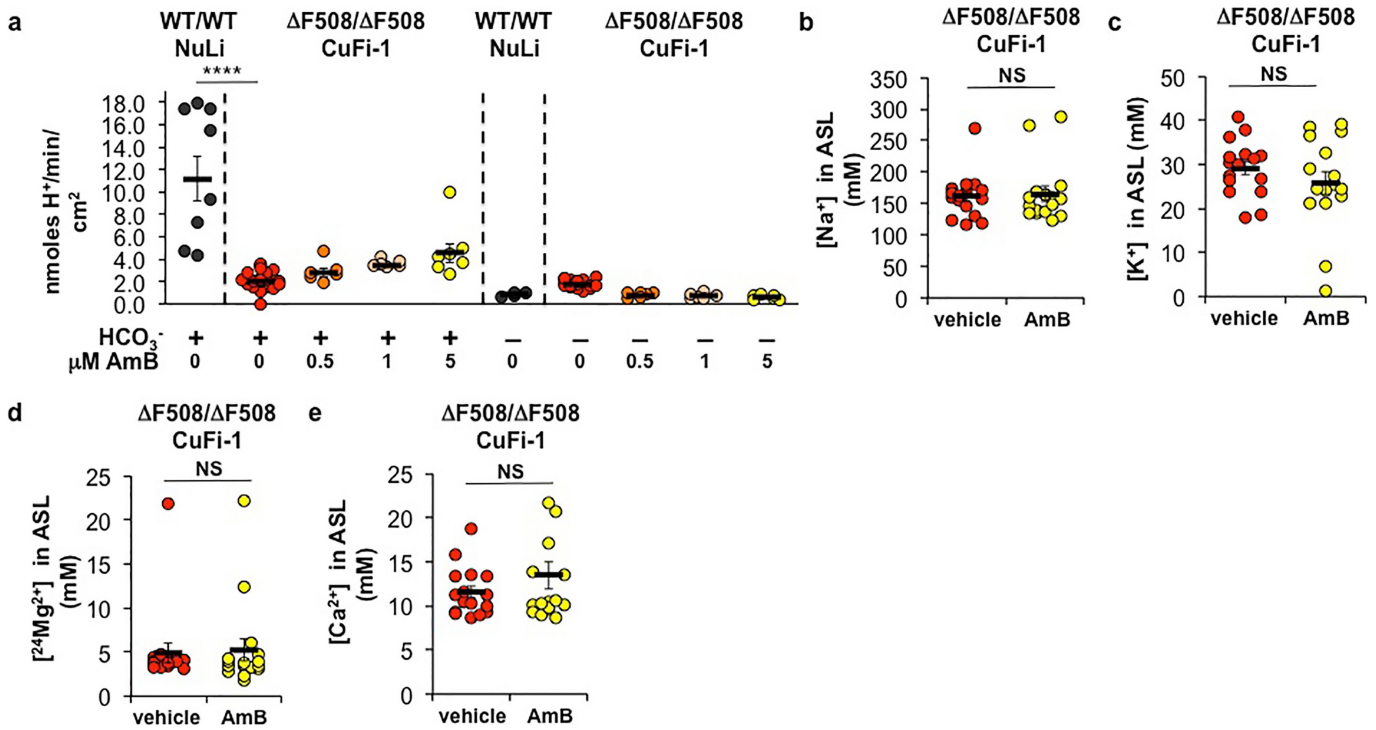

Extended Data Fig. 2 | AmB-mediated pH changes are HCO_3^--dependent and do not alter major cation concentrations in the ASL. a, Base secretion and acid absorption rates in NuLi (HCO_3^- +: $n = 8$ biologically independent samples; HCO_3^- −: $n = 4$ biologically independent samples) or CuFi-1 (ΔF508/ΔF508) epithelia (HCO_3^- +: $n = 23$ biologically independent samples, $P < 0.0001$; HCO_3^- −: $n = 18$ biologically independent samples) over 20 min after acute addition of increasing AmB concentrations, as measured by pH-stat titration. All n are biologically independent samples. HCO_3^- +: 0.5, 1 μM, $n = 6$; 5 μM, $n = 7$. 0.5 μM, $P = 0.9663$; 1 μM, $P = 0.7328$; 5 μM, $P = 0.1459$. HCO_3^- −: 0.5, 1, 5 μM, $n = 6$. The apical pH was titrated to a target pH of 6.0. **b**–**e**, The effect of AmB (2 μM) compared to perfluorocarbon (FC-72) vehicle after 48 h on Na^+ (**b**; $P = 0.7855$), K^+ (**c**; $P = 0.2892$), $^{24}Mg^{2+}$ (**d**; $P = 0.8339$) and Ca^{2+} (**e**; $P = 0.2708$ with Welch's correction) concentrations in the ASL in CuFi-1 (ΔF508/ΔF508), as measured by ICP-MS ($n = 16$ biologically independent samples). ANOVA (**a**), two-sided unpaired Student's t-test (**b**–**d**) or two-sided unpaired Student's t-test with Welch's correction (**e**) were used to assess statistical significance. Data are mean ± s.e.m.; NS, not significant; $^{****}P \leq 0.0001$. In all panels, measurements were taken from biologically independent samples.

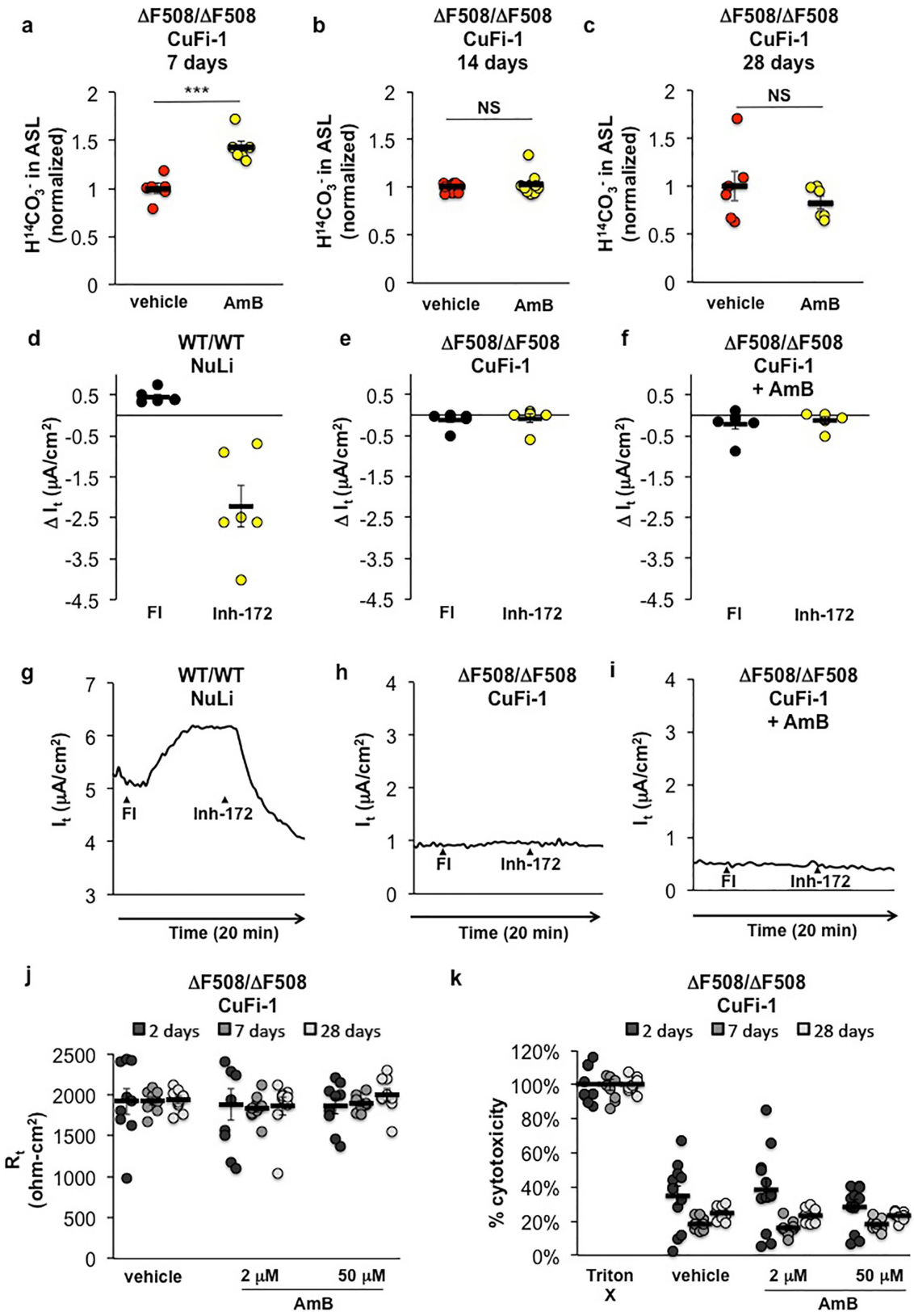

Extended Data Fig. 3 | See next page for caption.

Extended Data Fig. 3 | AmB treatment is sustained, is ineffective on wild type, is not due to increased CFTR activity, does not disturb membrane integrity, and is non-toxic. a–**c**, The effect of AmB (2 μM) compared to FC-72 vehicle left on the surface of CuFi-1 (ΔF508/ΔF508) epithelia for 7 (**a**; $n = 6$ biologically independent samples, $P = 0.0004$), 14 (**b**; $n = 9$ biologically independent samples, $P = 0.5138$) or 28 (**c**; $n = 6$ biologically independent samples, $P = 0.3421$) days on $H^{14}CO_3^-$ movement from the basolateral buffer to the ASL over 10 min after radiolabel addition, normalized to FC-72 vehicle addition. **d**–**i**, Changes in transepithelial current (I_t) after treatment with 10 μM forskolin/100 μM IBMX (FI) to activate CFTR and 1 μM $CFTR_{inh}$-172 to inhibit CFTR in NuLi ($CFTR^{+/+}$) epithelia (**d**, **g**), CuFi-1 (ΔF508/ΔF508) epithelia (**e**, **h**), and CuFi-1 epithelia treated with AmB (2 μM, 48 h) (**f**, **i**) ($n = 6$ biologically independent samples). **g**–**i** show a representative graph from six independent experiments repeated with similar results. **j**, Transepithelial electrical resistance (R_t) in CuFi-1 epithelia did not differ between treatment with vehicle or increasing doses of AmB over increasing time periods after a single treatment ($n = 9$ biologically independent samples). **k**, Cytotoxicity, as measured by detection of lactase dehydrogenase in CuFi-1 epithelia over increasing time periods after a single AmB or vehicle treatment, is represented as percentage of total cellular lysis by Triton X-100. AmB treatment did not cause increased cytotoxicity compared to vehicle ($n = 12$ biologically independent samples). In **a**–**c**, two-sided unpaired Student's *t*-test was used to assess statistical significance. In **a**–**f**, **j**, **k**, graphs show mean ± s.e.m.; NS, not significant; $***P \leq 0.001$. In all panels, measurements were taken from biologically independent samples.

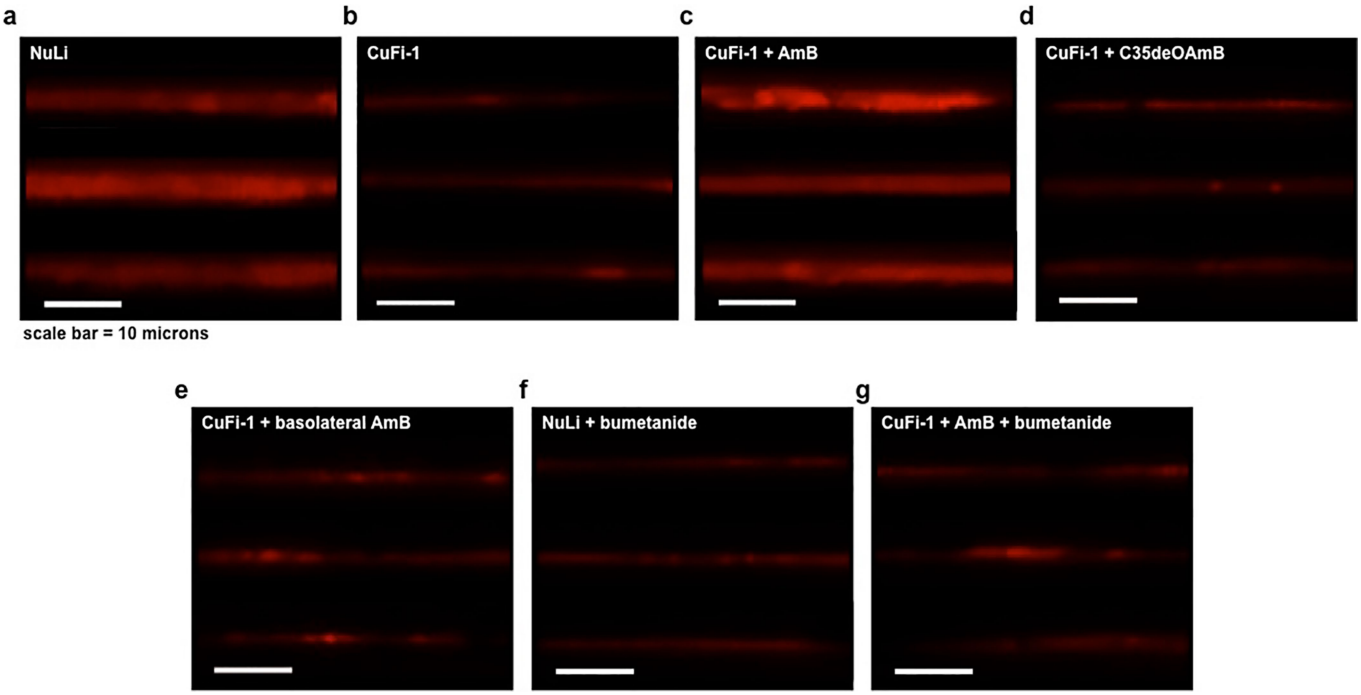

Extended Data Fig. 4 | AmB increases ASL height. ASL height, as imaged by confocal microscopy, in NuLi (*CFTR*$^{+/+}$) epithelia (**a**), CuFi-1 epithelia (**b**), CuFi-1 epithelia with apical addition of AmB (**c**), CuFi-1 epithelia with apical addition of C35deOAmB (**d**), CuFi-1 epithelia with basolateral addition of AmB (**e**), and NuLi (**f**) and AmB-treated CuFi-1 epithelia with basolateral addition of bumetanide (500 μM) (**g**). Representative images from at least six independent experiments are shown. In all panels, measurements were taken from biologically independent samples. Scale bars, 10 μm.

a

Patient #	Genotype	Trial 1 Δ pH	Trial 2 Δ pH	Trial 3 Δ pH
1	ΔF508/ΔF508	0.27	0.36	-
2	ΔF508/ΔF508	0.13	0.11	0.43
3	ΔF508/ΔF508	0.02	0.18	-
4	ΔF508/ΔF508	0.31	-	-
5	ΔF508/ΔF508	0.17	-	-
6	R553X/E60X	0.12	0.31	0.56
7	ΔF508/1717-1G→A	0.04	0.06	0.06
8	ΔF508/c.2052dupA	-0.16	0.14	-
9	D239G/V520F	0.68	0.15	-

d

Genotypes for ASL viscosity assay
ΔF508/ΔF508
ΔF508/ΔF508
ΔF508/ΔF508
ΔF508/c.2052dupA
ΔF508/Y563NPolyT
ΔF508/1717-1G→A

e

Genotypes for ASL antibacterial activity assay
ΔF508/ΔF508
ΔF508/ΔF508
ΔF508/ΔF508
ΔF508/ΔF508
ΔF508/ΔF508
ΔF508/ΔF508
D239G/V520F
ΔF508/1717-1G→A

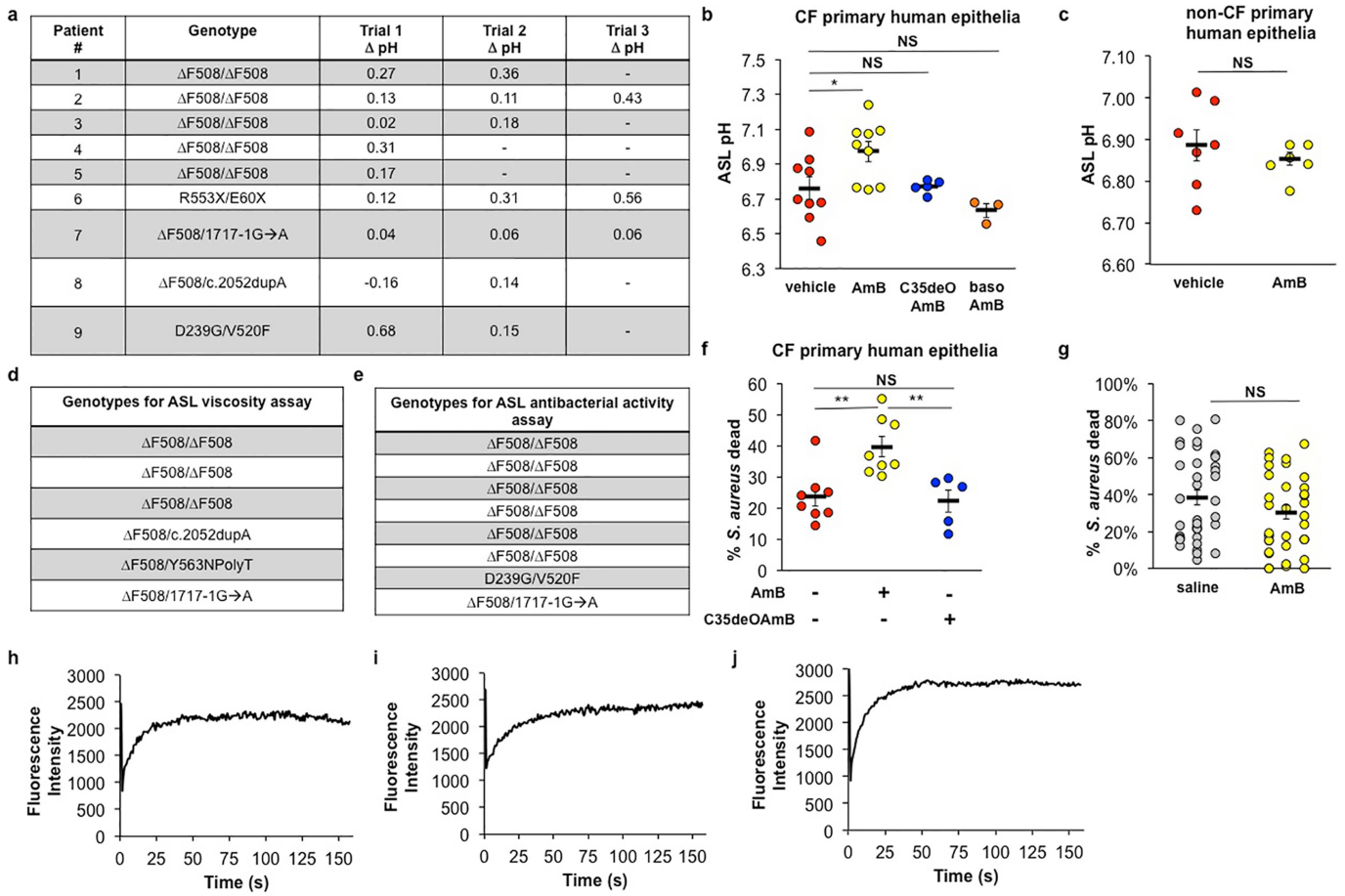

Extended Data Fig. 5 | AmB restores ASL pH and antibacterial activity in primary cultures of human airway epithelia from donors with CF. **a**, Genotypes and ΔpH measurements from patient donors in ASL pH assay. **b**, The effects of AmB (2 μM, 48 h; $n = 9$ biologically independent samples, $P = 0.446$), C35deOAmB (2 μM, 48 h; $n = 5$ biologically independent samples, $P = 0.9994$) and basolateral addition of AmB (2 μM, 48 h; $n = 3$ biologically independent samples, $P = 0.6359$) compared to vehicle on the average ASL pH of primary cultured airway epithelia derived from CF humans with different *CFTR* mutations. **c**, The effect of AmB (2 μM, 48 h; $n = 7$ biologically independent samples, $P = 0.4866$) compared to vehicle on ASL pH in non-CF epithelia. **d**, Genotypes of patient donors in ASL viscosity assay. **e**, Genotypes of patient donors in ASL antibacterial activity assay. **f**, The effect of AmB (2 μM, 48 h; $n = 8$ biologically independent samples, $P = 0.0042$) and C35deOAmB (2 μM, 48 h; $n = 5$ biologically independent samples, $P = 0.9626$) compared to vehicle on the average ASL antibacterial activity of primary cultured airway epithelia derived from humans with CF harbouring different *CFTR* mutations. Antibacterial activity is measured by the percentage of *S. aureus* killed after exposure to ASL. **g**, The ability of AmB (2 μM) alone to kill *S. aureus* compared to saline ($n = 36$ biologically independent samples, $P = 0.1569$). **h**–**j**, Representative FRAP traces for measuring ASL viscosity from six independent experiments repeated with similar results for non-CF (**h**), CF (**i**), and AmB-treated CF (**j**) epithelia. In **b** and **f**, ANOVA was used to assess statistical significance. Two-sided unpaired Student's *t*-test with Welch's correction (**c**) or two-sided unpaired Student's *t*-test (**g**) was used to assess statistical significance. Graphs show mean ± s.e.m.; NS, not significant; $*P \leq 0.05$; $**P \leq 0.01$. In all panels, measurements were taken from biologically independent samples.

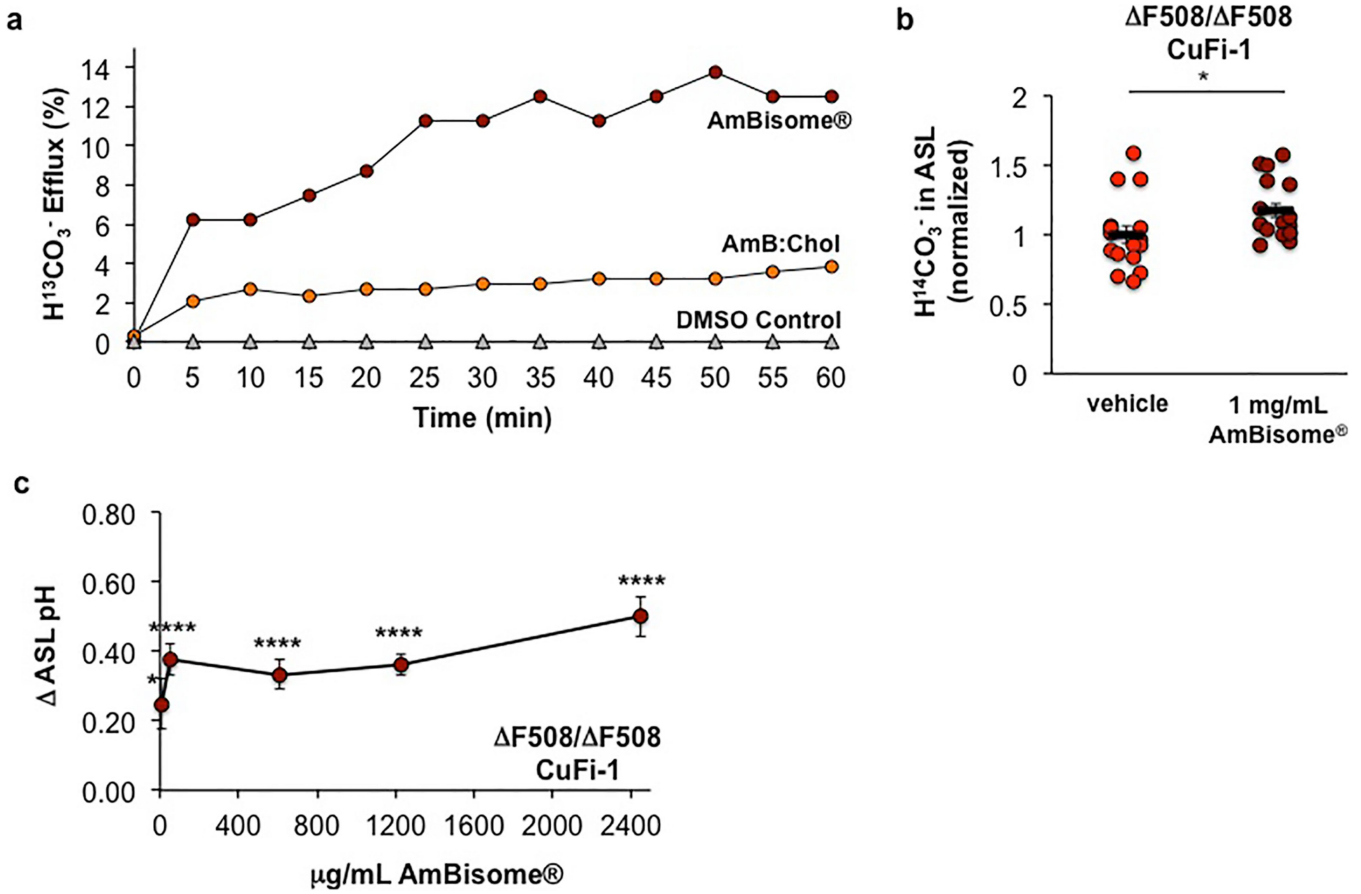

Extended Data Fig. 6 | AmBisome increases transepithelial $H^{14}CO_3^-$ secretion and ASL pH in a time- and dose-dependent manner. a, The effect of AmBisome (1:1,000 AmB:lipid ratio), AmB:cholesterol (1:1,000 AmB:lipid in DMSO), and sterile water or DMSO vehicle on $H^{13}CO_3^-$ transport across a POPC/10% cholesterol lipid membrane. **b**, The effect of AmBisome (1 mg ml^{-1}, 48 h; $n = 16$ biologically independent samples, $P = 0.0477$) compared to FC-72 vehicle on $H^{14}CO_3^-$ movement from the basolateral buffer to the ASL over 10 min after radiolabel addition in CuFi-1 (ΔF508/ΔF508), normalized to FC-72 vehicle addition. **c**, The effect of increasing AmBisome concentration (1 mg ml^{-1}, 48 h) compared to vehicle on ASL pH in CuFi-1 epithelia. All concentrations, $n = 9$ biologically independent samples; 0.25 μM, $P = 0.0106$; 2 μM, $P < 0.0001$; 25 μM, $P = 0.0002$; 50 μM, $P < 0.0001$; 100 μM, $P < 0.0001$. In **a**, a representative graph from at least three independent experiments is shown. In **b**, two-sided unpaired Student's *t*-test was used to assess statistical significance. In **c**, ANOVA was used to assess statistical significance. Graphs depict means ± s.e.m.; NS, not significant; $^*P \leq 0.05$; $^{****}P \leq 0.0001$. In **a**, the same sample for each replicate was measured repeatedly over time. In **b** and **c**, measurements were taken from biologically independent samples.

nature research

Corresponding author(s): Martin D. Burke

Last updated by author(s): Jan 29, 2019

Reporting Summary

Nature Research wishes to improve the reproducibility of the work that we publish. This form provides structure for consistency and transparency in reporting. For further information on Nature Research policies, see Authors & Referees and the Editorial Policy Checklist.

Statistics

For all statistical analyses, confirm that the following items are present in the figure legend, table legend, main text, or Methods section.

n/a	Confirmed	
☐	☒	The exact sample size (*n*) for each experimental group/condition, given as a discrete number and unit of measurement
☐	☒	A statement on whether measurements were taken from distinct samples or whether the same sample was measured repeatedly
☐	☒	The statistical test(s) used AND whether they are one- or two-sided *Only common tests should be described solely by name; describe more complex techniques in the Methods section.*
☐	☒	A description of all covariates tested
☐	☒	A description of any assumptions or corrections, such as tests of normality and adjustment for multiple comparisons
☐	☒	A full description of the statistical parameters including central tendency (e.g. means) or other basic estimates (e.g. regression coefficient) AND variation (e.g. standard deviation) or associated estimates of uncertainty (e.g. confidence intervals)
☐	☒	For null hypothesis testing, the test statistic (e.g. *F*, *t*, *r*) with confidence intervals, effect sizes, degrees of freedom and *P* value noted *Give P values as exact values whenever suitable.*
☒	☐	For Bayesian analysis, information on the choice of priors and Markov chain Monte Carlo settings
☒	☐	For hierarchical and complex designs, identification of the appropriate level for tests and full reporting of outcomes
☒	☐	Estimates of effect sizes (e.g. Cohen's *d*, Pearson's *r*), indicating how they were calculated

Our web collection on statistics for biologists contains articles on many of the points above.

Software and code

Policy information about availability of computer code

Data collection	Liposomal permeabilization data was collected using Orion Star Com. Confocal images were collected using ZEISS ZEN Black 2.0. Ussing chamber data was collected using Acquire and Analyze v.2.3. Plate reader data was collected using Biotek Gen5 v.2.05. Pig trachea pH data was collected using PreSens Measurement Studio. ICP-MS data was collected using QTEGRA.
Data analysis	Data and statistics were analyzed using Microsoft Excel for Mac 2011 v.14.4.4. Image data was analyzed using ImageJ v.1.48. NMR data was analyzed on MestReNova v10.0.

For manuscripts utilizing custom algorithms or software that are central to the research but not yet described in published literature, software must be made available to editors/reviewers. We strongly encourage code deposition in a community repository (e.g. GitHub). See the Nature Research guidelines for submitting code & software for further information.

Data

Policy information about availability of data

All manuscripts must include a data availability statement. This statement should provide the following information, where applicable:

- Accession codes, unique identifiers, or web links for publicly available datasets
- A list of figures that have associated raw data
- A description of any restrictions on data availability

All data are available in the manuscript or the extended data.

Field-specific reporting

Please select the one below that is the best fit for your research. If you are not sure, read the appropriate sections before making your selection.

☒ Life sciences ☐ Behavioural & social sciences ☐ Ecological, evolutionary & environmental sciences

For a reference copy of the document with all sections, see nature.com/documents/nr-reporting-summary-flat.pdf

Life sciences study design

All studies must disclose on these points even when the disclosure is negative.

Sample size	The sample size for each experiment is indicated in the figure legends. Based on pilot experiments, we chose sample sizes that adequately power each experiment to detect a difference in outcomes between groups. No statistical methods were used to predetermine sample size.
Data exclusions	No data was excluded from analyses.
Replication	To verify reproducibility of experimental findings, experiments were successfully independently replicated and data reproduced by 2-3 graduate student or post-doctoral researchers either from the Burke lab or the Welsh lab based on established protocols provided to each researcher.
Randomization	Epithelial samples and piglets were randomly allocated into experimental groups.
Blinding	All the measurements were performed by instruments or computing devices and therefore blinding is not necessary.

Reporting for specific materials, systems and methods

We require information from authors about some types of materials, experimental systems and methods used in many studies. Here, indicate whether each material, system or method listed is relevant to your study. If you are not sure if a list item applies to your research, read the appropriate section before selecting a response.

Materials & experimental systems

n/a	Involved in the study
☒	☐ Antibodies
☐	☒ Eukaryotic cell lines
☒	☐ Palaeontology
☐	☒ Animals and other organisms
☐	☒ Human research participants
☒	☐ Clinical data

Methods

n/a	Involved in the study
☒	☐ ChIP-seq
☒	☐ Flow cytometry
☒	☐ MRI-based neuroimaging

Eukaryotic cell lines

Policy information about cell lines

Cell line source(s)	The cell lines used in this this study were developed in 2003 by the Welsh Lab at the University of Iowa. Cell lines were generated using the reverse transcriptase component of telomerase, hTERT, and human papillomavirus type 16 (HPV-16) E6 and E7 genes to transform normal and cystic fibrosis (CF) human airway epithelial (HAE) cells. NuLi-1 (normal lung, University of Iowa) was derived from HAE of normal genotype and CuFi (cystic fibrosis, University of Iowa) were derived from HAE of various CF genotypes; specifically CuFi-1 was derived from ΔF508 HAE and CuFi-4 was derived from G551D/ΔF508 HAE.
Authentication	The original CF transplant donors were genotyped by Integrated Genetics (Westborough, MA). Cell lines were secondarily confirmed by the ATCC repository to have the correct genotype and were free of mycoplasma contamination. Development of the cell lines is detailed in the APS 2003 publication: https://doi.org/10.1152/ajplung.00355.2002.
Mycoplasma contamination	All cell lines tested negative for mycoplasma contamination.
Commonly misidentified lines (See ICLAC register)	No commonly misidentified lines were used.

Animals and other organisms

Policy information about studies involving animals; ARRIVE guidelines recommended for reporting animal research

Laboratory animals	We studied female and male newborn pigs with targeted disruption of the CFTR gene CFTR–/–, generated from mating CFTR+/–

Laboratory animals	pigs. Pigs were obtained from Exemplar Genetics.
Wild animals	The study did not involve wild animals.
Field-collected samples	The study did not involve field-collected samples.
Ethics oversight	The University of Iowa Animal Care and Use Committee approved all animal studies, and we have complied with all relevant ethical regulations.

Note that full information on the approval of the study protocol must also be provided in the manuscript.

Human research participants

Policy information about studies involving human research participants

Population characteristics	Airway epithelial cells were obtained from human trachea and bronchi of CF and non-CF specimens obtained from the Iowa Donor Network, either as post-mortem specimens or from tissue deemed not fit for transplant. All of the corresponding genotypes are indicated in the manuscript (see Extended Data Fig. 5). All samples were de-identified in the Cell Culture Core Repository and patient identification information was not provided to the researchers doing the experiments.
Recruitment	Patients were not recruited. Airway epithelial cells were obtained from human trachea and bronchi of CF and non-CF specimens obtained from the Iowa Donor Network, either as post-mortem specimens or from tissue deemed not fit for transplant.
Ethics oversight	Studies were approved by the University of Iowa Institutional Review Board.

Note that full information on the approval of the study protocol must also be provided in the manuscript.